THE CROSS-COUPLING PROBLEM OF HELICOPTER ROTORS - A REVIEW

Aviv Rosen*

Abstract

Until recently it was beyond the capability of helicopter rotor models to predict correctly the cross-coupling response. During the mid-nineties it became clear that wake distortion effects are the main contributors to the cross-coupling response. Wake distortion effects can be modeled by using detailed free or prescribed wake models. However, these models require large computer resources and long computing times, thus they are not suitable for various applications. In such cases dynamic-inflow models can be corrected to account for the missing effect, by using the wake distortion coefficient or an aerodynamic phase lag. Recently, a new actuator disk model was developed where the wake distortion effect is obtained as an integral part of the derivation. In the paper all the methods of considering the wake distortion effects are reviewed and compared. The results of the various models are also compared to flight test results. Conclusions are drawn and further necessary research is identified.

Nomenclature

C_T,C_{LA},C_{MA}	= aerodynamic thrust, roll-moment, and pitch-moment coefficients, respectively
g^j_{amp} (ω, K_R or ψ_a)	= expression describing the difference in amplitude between TEMURA's results and the corrected dynamic-inflow model, of the j^{th} response variable, at a frequency ω
g^j_{phase} (ω, K_R or ψ_a)	= expression describing the difference in phae angle between TEMURA's results and the corrected dynamic-inflow model, of the j^{th} response variable, at a frequency ω
I_{us}, I_{di}	= imaginary parts of the response variables obtained by TEMURA and the corrected dynamic-inflow model, respectively
K_R	= wake distortion coefficient
K_q,K_p (K_{Rc}, K_{Rs})	= pitch and roll wake distortion coefficients, respectively, in forward flight
$[L]^{-1}$	= aerodynamic matrix, Eq.(1)
$[L^1]^{-1}$,$[L^2]$	= Aerodynamic matrices, Eqs. (3b,c)
L_{qn}	= roll moment derivative with respect to pitch rate (N.m.sec/rad)
ℓ_1, ℓ_2	= aerodynamic coefficients, Eq.(3a)
lon	= longitudinal stick command
lat	= lateral stick command
[M],$[M^1]$,$[M^2]$	= aerodynamic "inertia" matrices, Eqs.(1), (3b), (3c)
M_{1c}',M_{1s}'	= "Lagged" aerodynamic pitch and roll moments (N.m)
M_{1c},M_{1s}	= "Unlagged" aerodynamic pitch and roll moments (N.m)
M_{qn}	= pitch moment derivative with respect to pitch (N.m.sec/rad)
M_1	= an aerodynamic coefficient in Eq.(3a)
p_D	= non-dimensional roll rate of the disk
p_f	= non-dimensional fuselage roll rate
q_D	= non-dimensional fuselage pitch rate of the disk
R_{us}, R_{di}	= real parts of the response variables obtained by TEMURA and the corrected dynamic-in-flow model, respectively
R	= rotor radius (m)
r	= non-dimensional radial coordinate
s	= Laplace variable

* Faculty of Aerospace Engineering, Technion - Israel Institute of Technology, Haifa 32000, Israel
Email : rosen@aerodyne.technion.ac.il

W^j_{amp}, W^j_{phase} = weighting factors of the amplitude and phase, respectively, of the j^{th} response variable, in the least-squares procedure

w_{zo}, w_{zs}, w_{zc} = coefficients of the nondimensional induced velocity, Eq.(4)

w_p, w_q = Non-dimensional induced velocity components due to wake distortion effects

w_f = non-dimensional perturbation in the downward velocity of the disk

β_o, β_s, β_c = constant, sine and cosine components of blade flapping

γ = lock number

ε = non-dimensional offset

λ = non-dimensional induced velocity relative to an inertial reference system

λ_o, λ_s, λ_c = non-dimensional components of the induced velocity through the disk, Eq.(2)

ν = non-dimensional induced velocity through the disk, relative to the disk reference system

τ_a = a time constant (sec)

ψ = Azimuth angle (sec)

ψ_a = aerodynamic phase lag (rad)

ψ_{au} = phase lag due to unsteady aerodynamics, including compressibility effects (rad)

Ω = rotor angular speed (rad/sec)

ω = frequency (rad/sec)

ω_β = first nondimensional flapping frequency

Symbols

$(\dot{})$ = differentiation with time

Introduction

The helicopter rotor is an unsymmetrical system because of its rotation. As a result of this asymmetry the rotor exhibits cross-coupling effects, namely: In addition to the main on-axis response to control input or maneuver, there is a secondary response in the opposite axis. Thus, for example, when the pilot pushes the stick forward the helicopter pitches nose down, but in addition it also rolls. Elementary blade-element models predict this coupling effect. Unfortunately, for many years the predictions of all the simulation models were opposite to flight test results or wind tunnel measurements. Thus, while the predictions of the off-axis response to the above push-over maneuver were rolling to the right, flight test results showed a left roll. Prouty [1] indicated that he faced such a problem in 1987 when he compared Apache flight-test maneuvers with computer predictions. No matter how the program was modified, the directions could not be reversed, and the problem remained unsolved.

Probably there were others who faced the same problem, but it seems that for many years people tried to ignore it. Only during the late 80's and beginning of the 90's did this problem start to attract increasing interest. Eshow et. al [2] compared A109 simulation and flight test results and indicated that while in the on-axis response close agreement was obtained, the off-axis response exhibited increasing discrepancies. Two years later, Harding and Bass [3] presented a validation study of a flight simulation model of the AH-64, by comparing its results to flight-test data. They indicated deficiencies in correlation for pitch to roll and roll to pitch cross-coupling. Similar conclusions followed the validation of an UH-60 simulation model in hovering flight [4] The authors' concluded that, "The accurate representation of all off-axis response characteristics is beyond the capability of current-generation (written in 90-91) real-time rotorcraft simulations. A realistic goal is to correctly model any cross-coupled responses that are of sufficient magnitude to affect pilot reaction or workload, or that contribute to the cue environment of the pilot".

The cross-coupling mystery [as it was named by Prouty in Ref.1] continued to attract the interest of various researchers. Chaimovich et al. [5] presented correlations between flight test results and numerical simulations for an AH-64, showing the large discrepancies in the case of the off-axis response. Curtiss [6] in a similar study of both the AH-64 and UH-60, concluded that the most difficult difference to explain is the off-axis response, which in all the cases that he considered resulted in theoretical predictions that were basically opposite to experimental ones. Fletcher [7] reached a similar conclusion when he investigated the flapping characteristics and angular response of an UH-60.

While all the above-mentioned studies referred to flight-test data, Tischler et al.[8] studied the dynamics of a Sikorsky Bearingless Main Rotor (SBMR) from frequency response wind tunnel test data. They showed that adjustment of the swash plate control phasing was needed in order to match simulation results and the wind tunnel data.

The various studies, including different rotors at different operating conditions, indicated that a certain important effect is missing in all the simulation models. This led many researchers to look for physical effects that could cause the cross-coupling mystery.

Various researchers studied the influence of blade flexibility on the phenomenon. He and Lewis [9] used a finite-state dynamic wake model, combined with an elastic model of the blades. Although the on-axis response was improved in certain cases, they concluded that the correlation of the off-axis response to the flight test was not as good as the on-axis response. Sturisky and Schrage [10], using a different model and a different approach, arrived at a similar conclusion. Turnour and Celi [11] developed a flight dynamic simulation model that included rotor blade flexibility. Their results indicated that refining the main rotor model by including blade flexibility does not improve the prediction of the off-axis response to pilot inputs.

Grnhagen [12] extended the DLR helicopter simulation program to include effects of changes in the inflow angular momentum due to downwash rotation, which he called "virtual inertia effect". After comparisons with flight tests he concluded that including this effect significantly improves the prediction capability of pitch-roll cross-coupling.

All efforts to solve the cross-coupling mystery indicated that the off-axis response is very sensitive to various effects, but an increasing number of researchers felt that the main cause of the discrepancy between theoretical modeling and flight test results is a missing aerodynamic phenomenon.

Wake Distortion Effects-Vortex Modeling

Isser and Rosen [13] presented the derivation of a new model of the unsteady aerodynamics of a hovering helicopter rotor. The model was called TEMURA - TEchnion Model of Unsteady Rotor Aerodynamics. This is a prescribed wake model that includes the bound vortices along the blades, as well as trailing and shed vortices. Harmonic perturbations about hover are considered and the variations of the induced velocities and aerodynamic loads along the blades are calculated. The new model was investigated by comparing it to previous models [14]. It also exhibited good agreement with experimental results for the flapping response of rotor blades to collective and cyclic pitch inputs [15], or the coupled free vibrations of rotor flapping and body pitch and roll in hover [16].

A new phenomenon was included in TEMURA that in Ref. 13 was called geometric effects, and is now known as wake distortion. As a result of spatial motions of the blades, the path of vortex elements that leave the trailing edges of the blades and form the wake, differ from the path of the vortex elements that leave the same cross-sections during a steady hover. Thus the wake geometry of a rotor performing maneuvers is different from the wake geometry of the same rotor during a steady hover, leading to naming the phenomenon "wake distortion". Variations in the wake geometry result in variations in the induced velocities along the blades and as a result also variations in the aerodynamic loads along the blades.

In a prescribed wake model the wake geometry is based on certain assumptions that determine the path of vortex elements that leave the trailing edges of the blades and float downstream. The wake distortion effects depend on these assumptions. In TEMURA two options exist:

(a) It is assumed that each vortex element follows a path identical to the path of a vortex element that leaves the same cross-section during steady hover. This path is measured relative to a rotor axis that is normal to the disk at the moment when the vortex element leaves the blade's trailing edge. Since the disk pitches and rolls, the direction of this axis changes with time.

(b) It is assumed that each vortex element follows a path identical to the path of a vortex element, which leaves the same cross-section during steady hover. This path is measured relative to the rotor axis in the steady hover case. The difference between this case and a steady hover is that there is, in general, a difference in the inertial location of the point where the vortex element leaves the blade's trailing edge. This is due to the disk motion and rotation.

In Fig.1 the distorted wake of a rotor during steady pitch is shown, based on the above two assumptions. For the sake of clarity contraction has been neglected and a constant axial velocity of all the vortex elements is assumed. It is shown that according to assumption (a) a curved vortex tube is obtained, where on one side the vorticity density increases, while it decreases on the other. According to assumption (b) the vortex tube is not curved, but there is a change in the vorticity density on both sides of the tube.

It is reasonable to assume that for the case of a "steady" slow pitch or roll, assumption (a) should be adopted. This is probably also the case at low frequencies of the perturbations. As the frequency of the perturbations increases, it is reasonable to assume that the actual situation is somewhere between assumptions (a) and (b). In most of the previous investigations, which will be reviewed in what follows, the case of a steady pitch or roll was analyzed, and therefore most of them used assumption (a). It seems that it is justified to use assumption (a) in most analyzes, since at high frequencies of the perturbations the influence of wake distortion becomes smaller and thus inaccuracies in the assumption results in only a small effect. Nevertheless a mechanism combining options (a) and (b) can be used.

In Ref.[17] a rotor of a hovering helicopter, during steady pitch or roll perturbations, was investigated. The on-axis stability derivative, M_{qn} (pitch moment derivative with respect to pitch rate), and off-axis stability derivative, L_{qn} (roll moment derivative with respect to pitch rate), were calculated. It was shown that unsteady aerodynamic effects (other than wake distortion) affect the on-axis results and to a less extent the off-axis results. When it comes to wake distortion (denoted geometric effects in the paper), its effect on the on-axis derivative is negligible, while it has a significant influence on the off-axis derivative. Both, M_{qn} and L_{qn}, were calculated as functions of the nondimensional blade offset. It was shown that for the AH-64 a change of sign in L_{qn} is obtained as a result of including wake distortion effects. Thus it was shown for the first time that wake distortion could explain the cross-coupling mystery.

To examine the physical phenomenon, imagine a rotor in steady pitch motion (nose-up). As a result of the wake distortion shown in Fig.1 (either assumption (a) or (b)) there will be an increase in the induced velocity over the rear part of the disk, and a decrease over the front part, relative to the steady hover case. The maximum change will be along the longitudinal axis and will decrease as the distance from this axis increases. Due to the classical lag of 90° of a flapping blade, this longitudinal change in the induced velocity is translated into a contribution to a right tilt of the disk, exactly what was observed in flight tests.

In the case of a rigid rotor, the lag of 90° does not exist. Thus wake distortion will affect the on-axis response. Takasawa [18,19] measured the pitch damping of models of rigid helicopter rotors in hover. The results indicated that the measured pitch-damping derivative was less than one third of the classical theoretical value, when the rotor rotational speed was small compared to the first natural bending frequency of the blade. The results confirmed previous observations by other researchers. After different unsteady aerodynamic models could not solve the problem, Takasawa [18, 20] developed a quasi-steady three-dimensional aerodynamic model that included a trailing vortex sheet of the returning wake and accounted for the relative position between the blade and the trailing vortices in the returning wake. Thus this model included simple wake distortion elements. The new model showed a decrease in the damping, but still predicted values that were much higher than the measured values (overprediction between 20% and 150%). TEMURA was applied [Ref.21] to the cases reported by Takasawa and showed good agreement with the experimental results.

At the beginning TEMURA included only blade pitch angles as input, and blade flapping, fuselage pitch and roll, as output. During the years the code has been extended to include fuselage yaw and lateral motions, as well as additional effects such as compressibility [Ref.22].

In Figs. 2a,b the results of TEMURA for the frequency response of a hovering UH-60 are compared with flight test results. The results of three different simulation models are presented.

- "Steady" aerodynamics - Perturbations in the induced velocity due to perturbations in the wake vorticity (including trailing and shed vortices) or wake geometry (wake distortion) are not included.

- A model that does not include wake distortion - All the perturbations in the induced velocity due to variations in the intensity of the trailing, shed and bound vortices, are included, except for wake distortion effect.

- A complete model.

It is shown that the "steady" aerodynamic model exhibits large deviations from the amplitude of the on-axis flight-test results as the frequency is decreased. The off-axis results of model (a) exhibit large deviations in amplitude (especially in the case of q_f/lat) and significant differences in phase, of the order of 180°, along wide ranges of frequencies.

Adding variations in the induced velocity namely unsteady aerodynamic effects, but still not including wake distortion effects, has a similar effect to including a dynamic-inflow model. Except for very low frequencies, there is a good agreement between the simulation and flight test results of the on-axis response. There still exist large deviations, in amplitude but especially in phase, in the case of the off-axis response.

When the complete TEMURA model, that includes the wake distortion effects, is used, a significant improvement is seen. In the case of the on-axis response a very good agreement in amplitude at low frequencies, is obtained at the price of a somewhat increasing deviation of the phase at that region. Concerning the off-axis response, there is a very good agreement in phase and the 180° deviation disappears. The amplitude of (q_f/lat) shows a good agreement. The amplitude of (p_f/lon) displays trends similar to the flight-test results, showing a minimum at 2-3 rad/sec, but there are deviations in amplitude that increase at low frequencies. Overall TEMURA exhibits a very good agreement with the flight test results.

Various researchers followed the approach of TEMURA and used prescribed wake models to calculate the wake distortion coefficient. These papers will be reviewed in section Actuator Disk Models.

Since the wake distortion effects are associated with the wake geometry, it is clear that free wake analyses offer a strong tool to investigate these effects. While prescribed wake models are based on certain assumptions (concerning the wake geometry) that may result in errors when they are inaccurate, the geometry of the wake of a free wake analysis is obtained as a result of basic physical laws.

Keller and Curtiss [23] used a free wake method to investigate the induced velocity due to pitch rate superimposed on a basic state of hover or forward flight. Preliminary results illustrated the wake geometry and induced velocity variations, which occur when the rotor is pitching. However, the authors also reported numerical problems in the modeling procedure.

Bagai, Leishman and Park [24] presented a free-vortex model of a rotor undergoing steady maneuvers. The wake model was based on a finite-difference approximation of the vorticity transport equation. It was shown (as expected) that maneuvers are a source of additional distortion to the wake. This wake distortion can be sensitive to the maneuvering rates. The authors found that the wake distortion manifests as a counter intuitive change in the induced velocities over the disk that becomes a contributor to the "off-axis" response of the rotor. Park and Leishman [25] added to the model of Ref.24 a few models of unsteady cross-sectional aerodynamics. The results indicated that the effects of unsteady aerodynamics on the predictions of the rotor wake geometry and inflow are relatively small, and are unlikely to be a primary contributor to the off-axis response. Leishman, Bhagwat and Bagai [26] presented further results of free-vortex filament methods applied to analyze a rotor at a steady pitch rate, at hover and forward flight.

Theodore and Celi [27] used Bagai and Leishman's model in a code that describes coupled rotor-fuselage flight dynamics. This aerodynamic model was coupled with an elastic model of the blades. Good agreement between the results of the model and flight test results of a BO-105 at 17 knots, were presented. It was shown that wake distortion has a significant influence on the off-axis response, but in order to obtain good correlation, it is also important to include elastic torsion.

While most of the initial investigations concentrated on steady maneuvers, Bhagwat and Leishman [28] presented an investigation of a time-accurate free-vortex method to predict the evolution of the rotor wake aerodynamics during transient, maneuvering flight conditions. After verification of the methodology, it was applied to study maneuvering flight problems consisting of both sudden and steadily imposed angular pitch and roll rates. It was shown that time-dependent effects associated with maneuvers induced wake distortion, significantly influence rotor aerodynamics. Spatial and temporal lag was found in the build-up of the rotor inflow because of the dynamic growth and convection of vorticity in the rotor wake. The magnitude of the maneuver induced wake distortion effects was found to vary with rotor operating conditions as well as with rotor geometric parameters such as the blade flapping frequency. In a later work Ananthan and Leishman [29] used the same model to predict the evolution of the rotor wake and corresponding unsteady blade loads in response to time-varying changes in blade pitch. Both, steady and maneuvering flight conditions were examined. Recently the same authors [Ref.30], investigated the wake dynamics of a helicopter undergoing large amplitude, high rate maneuvering flight conditions. Five different tactical maneuvers were studied. Overall the results demonstrated the large nonlinear wake dynamics that would be produced during combat-like flight maneu-

vers and the necessity of using a rotor wake model with spatial and temporal resolution.

Another simplified free wake model was developed at ONERA [Refs.31,32]. In this model the trailing vortices produced during one rotor revolution, are represented by a group of concentric and coplanar vortex rings. In the plan of each group of vortex rings, radial segments are added between two azimuth directions occupied by the blades, in order to model shed vortices. Each vortex group is convected away from the rotor by the resultant fluid velocity across the rotor at the time of the vortex ring emission.

Basset and Tchen-Fo [32] reported that during steady pitch or roll the inflow gradients in the first harmonic approximation were highly linear. So they used their model to calculate the wake distortion coefficients in section - actuator disk models. For modeling of the wake distortion effects during time simulations the authors suggested two methods: One, which is suitable for real time application, uses the wake distortion coefficients and is based on a wide database and a neural network scheme. The other is based on a continuous closed-loop simulation of the wake geometry.

Graham and Katz [33] presented another free wake model that was used to study the wake distortion effect.

Actuator Disk Models

Free wake models or even prescribed wake models require very large computer resources and long computing times, thus they are not suitable for many purposes, like for example flight mechanics simulations. Actuator disk models on the other hand, are very useful for applications where efficiency is required. Among the actuator disk models, probably the most popular is the dynamic-inflow model of Pitt and Peters [34]. It describes a three-state unsteady rotor inflow distribution that is governed by the rotor thrust, as well as the aerodynamic pitch and roll moments. This model was later on extended to the Finite State Unsteady Wake Model [35], that includes higher harmonic functions for azimuthal load distribution (compared to the three functions of the dynamic-inflow model), as well as higher number of radial shape functions described by Legendre polynomials. Originally the dynamic-inflow model did not include the effect of wake distortion. After Rosen and Isser [17] pointed out the important influence of this effect, Keller [36] added it to the dynamic-inflow model by introducing the wake distortion coefficient, K_R. In order to calculate K_R the author replaced the rotor with an infinite number of blades with constant bound circulation, after neglecting wake contraction a vortex tube was obtained. For the cases of steady pitch or roll rates in hover, this vortex tube is curved. Keller replaced the tube with a series of vortex rings and calculated the perturbation in the induced velocity over the disk, due to the curvature that is directly related to the pitch or roll rates. In an analog manner to the dynamic-inflow model, he fitted this perturbation of the induced velocity with linear sine and cosine distributions. It was found that for small rates the coefficients of the linear cosine and sine distributions, are functions of the pitch and roll rates, respectively, and are independent of the tip vortex strength. The coefficient was denoted K_R and its value was calculated to be 1.5. By introducing this parameter into the model, the off-axis results for a hovering UH-60 were improved significantly, while the influence on the on-axis response was negligible.

In another paper Arnold et al. [37] used a system identification technique to determine the value of K_R from flight data of an UH-60 in hover. The identified value was 3, twice the theoretical value of 1.5 [Ref.36].

Following the results obtained by Keller [36] and Arnold et al. [37] various researchers used different approaches to calculate K_R.

In [Ref.38] momentum theory was used to calculate the coefficient. For a fast axial flight a value of one was obtained, that reduces to 0.5 in the case of hover.

Most of the researchers used vortex models to obtain the value of K_R. Barocela et al.[39] used a vortex lattice model. For a vertical climb (axial flight) they obtained a value of $K_R = 1$, which agrees with the results of the momentum theory in Ref.[38]. For hover wake contraction was included in the vortex lattice modeling, using empirical models of wake geometry, obtained from the literature. They found that in hover the curved contracted wake results in a reduction of K_R (compared to axial flight) to 0.5, a result that also agrees with the momentum theory. However, there is an effective doubling of the wake curvature that offsets the reduction in K_R.

In Ref.[40] Krothapalli et al. derived a generalized model for wake distortion in hover, using the exact results of a vortex tube theory. They obtained a value of K_R=1 and explained that the difference with Keller's value ($K_R = 1.5$) is due to the constant curvature assumption of

Keller. It was also indicated in Ref.[40] that after using the vortex lattice model of Ref.[39] for 3, 4 and 5 bladed rotors, the average effective value for K_R was found to be approximately 1.33. This value was determined by calculating the effective moment on the rotor blade rather than calculating the coefficient of the radial inflow distribution.

In Ref.[41] the authors continued to emphasize the important influence of the wake contraction in hover on the effective curvature of the distorted wake due to pitch or roll rates. They used a value of $K_R = 1.33$ and presented a formula to introduce the effect of forward flight (skew angle of the wake) on the wake distortion effect. The K_R approach was combined with a generalized wake model and the results of the extended model showed good agreement with wind tunnel flapping results of the SBMR. The studies also showed that the inclusion of more than three states in the model does not offer a significant improvement. In Refs.[42] and [43] Peters, Prasad and their students presented reviews of their extensions, of the dynamic-inflow model and the Finite State Dynamic Wake Model, including the addition of wake distortion effects. In Ref.[43] the interaction of hinge offset effect and wake curvature effect on the off-axis response was studied. The results suggested that as the hinge offset increases, off-axis response magnitude increases while wake curvature effects decrease.

Free wake analyses, which were mentioned above, were also used to calculate K_R. Basset and Tchen-Fo [32] presented calculated K_R values in hover, vertical climb and forward flight. In forward flight the symmetry of axial flow (hover or vertical climb) is lost and thus two different coefficients are used for wake distortion effects due to pitch or roll (K_q and K_p, respectively). In general, the wake distortion effects decrease as the flight velocity increases. The detailed investigation in Ref. [32] includes also studies on the influence of thrust coefficient, center of rotation location and vertical speed component. For hover the authors obtained a value of 1.6 that is very close to the 1.5 reported by Keller. Park and Leishman [25], using their free wake model, calculated K_R for hover and K_q in forward flight. In their calculations they used a simple linear representation of the inflow and compared it with a higher harmonic representation. There were large differences between the two representations at low advance ratios. Steady pitch was considered and at forward flight the pitch rate direction exhibited a significant influence on the value of K_q. At hover an average value of $K_R \approx 2$ was obtained, while the results were somewhat dependent on the pitch rate and blade lift distribution caused by blade twist. Recently Bhagwat and Leishman [28], using their free-vortex wake model, reported that the wake distortion coefficient, in addition to variations with rotor thrust, also varies with other rotor parameters like the blade flapping frequency (hinge offset). In forward flight the effects of wake distortion were found to vary significantly with both, the advance ratio and the imposed maneuver rate.

Using the K_R coefficient to account for wake distortion effects is very convenient since many simulations already include dynamic-inflow models. The extension of these models to also include the K_R terms is straightforward.

Since there are differences between the wake distortion coefficient values reported by various researchers, investigations on the sensitivity of the results to the value of K_R and efforts to find its optimal value were carried out.

Keller and Curtiss [44] used a rigid wake model to calculate the induced velocity for a rotor undergoing steady pitching motion. They found, in agreement with the results of Ref. [24], that in hover the induced velocity variation due to angular rate is linear and may be approximated by the simple dynamic-inflow expansion. Results in forward flight, however, demonstrated a more complex flow field that requires additional inflow "modes" to capture the complete influence of angular rate. The authors used a five-term expansion retaining inflow coefficients to the second harmonic. They also obtained five wake-distortion coefficients, associated with the inflow coefficients, and showed their magnitude as a function of advance ratio. Except for an increase at very low advance ratios, those coefficients decreased rapidly with advance ratio.

Keller and Curtiss also investigated the damping in pitch of a rigid rotor, the same case that was studied in Refs.[18-21]. They found that a value of $K_R = 1.1$ gave the best correlation with the test results. This value is lower than the $K_R = 1.5$ obtained in their previous analyses.

Tischler [45] used the wind tunnel results of the SBMR (Sikorsky Bearingless Main Rotor), at 40 knots and 100 knots, to identify the wake distortion coefficients. He referred to K_{Rc} and K_{Rs}, instead of K_q and K_p, respectively. After using CIFER for identification, he found that K_{Rc} was insensitive and thus it was set to zero. This result was consistent with the computations of Ref. [44] that indicated that the longitudinal distortion effect is largely washed-out beyond $\mu = 0.06$. At 40 knots the lateral

distortion coefficient, K_{Rs}, was equal to 0.581, a significant reduction from hover, which is consistent with washout trends at increasing advance ratios as reported in Ref. [44]. The wake distortion effect at 100 knots was negligible.

Various groups of researchers and engineers extended the dynamic-inflow models in their simulation codes, to also include wake distortion effects through the use of the wake distortion coefficient. Hamers and von Grunhagen [46] obtained good correlation between simulation and flight test results of a BO-105, especially for the off-axis response, when a value of $K_R = 1.5$ was chosen for hover and decreased linearly to a value of $K_R = 1$ at 80 knots. He Chengjian et al. [47] extended the Peters-He Finite State Dynamic Wake Model to include wake distortion effects through the use of K_R. They used a vortex wake model to calculate K_R and obtained a value of 1.2. Their simulations showed that the inclusion of wake distortion effect corrected the wrong trend of the off-axis response. The simulation results, however, still underestimated the magnitude of the off-axis response.

Theodore and Celi [27] compared results obtained using various values of K_R with flight test results of a maneuver of a BO-105 near hover. While the on-axis response was very little affected by K_R, the off-axis response was significantly improved by introducing K_R. At different stages of the maneuver different values of K_R gave the best correlation with flight test results. The best overall correlation among various values of K_R seemed to occur for K_R= 1.5. The off-axis response is sensitive to other effects [Ref.48] and the authors showed the interaction between blade flexibility and the wake distortion effects, but it was clear that the wake distortion effects presented the major influence. The authors also concluded that the free wake model that they used, which was mentioned above, predicts the off-axis response more accurately than the dynamic-inflow model with the wake distortion coefficient.

In Ref. [49] a case of an isolated articulated rotor was studied using a regular value of K_R and the results were compared with wind tunnel results. The effect of wake distortion was found to be small and the amount of coupling was underestimated compared to what would be needed to improve the correlation between the calculations and wind tunnel results. On the other hand, at the same conference, Hamers and Basset [50] presented comparisons between results of simulations and flight test results of a BO-105 and a Dauphin. In the simulations they used the Pitt and Peters' dynamic-inflow model and the more complicated Finite State Unsteady Wake model. For both models the wake distortion coefficient at hover was taken equal to 1.5 and gave good results in comparison with flight test results of a BO-105. For a BO-105 flying at 100 knots and performing a longitudinal maneuver, values of $K_p = K_q = 0.5$ were used. These coefficients were higher than the theoretical values derived for that forward speed (which are close to zero); however they allowed a better off-axis prediction. For a Dauphin flying at 90 knots and performing a Dutch-roll, good agreement with the off-axis flight test results was obtained with $K_p = 0.5$ and $K_q = 0$.

Smith [51] used K_{Rc} and K_{Rs} (K_q and K_p) in the simulation of a S-76C. These coefficients, as well as other gains, were defined so that the characteristics of the simulation will match those of a real flight.

Researchers from DLR and ONERA [Refs. 52, 53] used advanced system identification methods to identify K_p and K_q from flight test results of a BO-105. It is interesting to note that even for hover, where both coefficients are expected to be equal, different values were obtained, probably as a result of fuselage aerodynamic characteristics. While a certain analysis result in: $K_p = 2.3$ and $K_q = 1.7$, another analysis gave $K_p = 2.5$ and $K_q = 1.6$. The average value of both analyses is $K_R \equiv 2$. In forward flight (40 m/sec) values of $K_p = 1.1$ and $K_q = 1.6$ were identified. It was shown that using these values in various simulations, resulted in significant improvement in the agreement between the calculated and measured results.

Zhao, Prasad and Peters [Refs. 54-56] presented an improved dynamic wake distortion model that included the effects of: longitudinal and lateral wake curvature, wake skew and wake spacing. Additional effects were also modeled. Simulations showed that the agreement between the calculated results and flight test results, are improved significantly as a result of introducing the various effects.

The common form of the dynamic-inflow equations, extended to include wake distortion effects, is:

$$\frac{1}{\Omega}[M]\begin{Bmatrix}\dot{\lambda}_o\\ \dot{\lambda}_s\\ \dot{\lambda}_c\end{Bmatrix} + [L]^{-1}\begin{Bmatrix}\lambda_o\\ \lambda_s\\ \lambda_c\end{Bmatrix} = \begin{Bmatrix}C_T\\ C_{LA}\\ C_{MA}\end{Bmatrix}$$

$$+\frac{1}{\Omega}\begin{bmatrix}0 & 0 & 0\\ 0 & K_p & 0\\ 0 & 0 & K_q\end{bmatrix}[L]^{-1}\begin{Bmatrix}0\\ p_f-\dot{\beta}_s\\ q_p-\dot{\beta}_c\end{Bmatrix} \quad (1)$$

where the nondimensional induced velocity distribution through the disk is

$$\lambda = \lambda_o + \lambda_s r\sin\psi + \lambda_c r\cos\psi \quad (2)$$

[M] and $[L]^{-1}$ are the regular matrices of Pitt and Peters' dynamic-inflow model. C_T, C_{LA} and C_{MA} are the rotor aerodynamic thrust, roll moment and pitch moment, coefficients, respectively. β_s and β_c are the first sine and cosine components of blade flapping, while p_f and q_f are the fuselage (shaft) roll and pitch rates, respectively. Ω is the rotor angular speed. K_p and K_q in Eq. (1) are the wake distortion coefficients for roll and pitch, respectively, that become identical at hover and usually denoted K_R. As indicated above, in certain references K_p and K_q are replaced by K_{Rs} and K_{Rc}, respectively.

The results of using Eq. (1) in a simulation of the frequency response of an UH-60 in hover, are shown in Figs. 3a,b.

Figure 3a presents the on-axis response. Results for five values of K_R (0, 1, 1.5, 2 and 3) are shown. $K_R = 0$ represents the results of a regular dynamic-inflow model without any wake distortion effects. It is shown that only at low frequencies (usually less than 1 rad/sec) and at high frequencies (greater than 10 rad/sec), K_R has an influence on the on-axis response. It is interesting to note that at low frequencies increasing values of K_R improve the agreement of the simulation results with the amplitude of the flight test results, but at the same time $K_R = 3$ tends to show large deviations from the phase of the flight test results.

Figure 3b presents the off-axis response. In the case of pitch rate response to lateral command (q_f/lat), the results of $K_R = 0$ show large deviations from the flight test results in amplitude and phase (the well known 180° difference in phase). All the other cases where $K_R \geq 1$ exhibit the correct phase. As K_R increases the agreement of the amplitude also improves. The K_R = 2-3 cases exhibit good agreement in amplitude. The results for roll response to longitudinal command (p_f/lon) show that the difference of 180° for frequencies lower than 2 rad/sec disappear for $K_R \geq 1.5$. The reader should not be misled by what seems to be a bad agreement, between the phase as obtained by simulation and flight test results, for frequencies larger than 2.5 rad/sec. This difference is 360°. The phenomenon, where the phase angle increases instead of decreases, at the range of 1.5-2.5 rad/sec, was discussed by Mansur and Tischler [57] and explained as an influence of a pair of lightly damped complex zeros. By following the approach presented in Ref. [57] of correcting this zero from minimum phase to non-minimum phase, a good correlation between the calculated and measured phase can be achieved. Concerning the amplitude of (p_f/lon), for frequencies lower than 2 rad/sec, good agreement between flight test and simulation results is obtained for $K_R = 2$ (this is also true for the phase angle). For frequencies higher than 3 rad/sec, as K_R is increased, the deviations between the measured and calculated amplitudes increase.

This dependency on frequency of the K_R value that gives the best agreement with flight test results is not new. Although the first versions of TEMURA included the influence of frequency, most of the later investigations assumed constant pitch or roll rates. Thus almost all the calculations of K_R were based on the assumption of steady pitch or roll. Curtiss [58] pointed out the importance of modeling the transient behavior of a rotor wake, but did not present a model that dealt with this issue. As indicated above, Bhagwat and Leishman [28] pointed out, based on using a free wake analysis, that time-dependent effects associated with maneuver induced wake distortion, significantly influence rotor aerodynamics. At the same time Prasad et al. [43], in order to incorporate the transient dynamics of the wake curvature in their analysis, represented the variations of K_p and K_q by a first order ordinary differential equation, which means two additional states (and equations) to the system of Eq. (1). After using a free wake analysis they obtained time constants associated with the dynamics of K_p and K_q, that are roughly three times larger than the time constants of the regular inflow dynamics.

The results of Figs. 3a,b clearly point out that the value of K_R that gives the best correlation between theory and flight test results, is frequency dependent. In order to find

this value in a systematic manner, a numerical procedure of optimal matching, based on a least-squares procedure, was developed and is described in Appendix-A. At each frequency matching is performed on the four response variables of interest: (q_f/lat), (q_f/lon), (p_f/lat), (p_f/lon). Since each response variable includes amplitude and phase, there are eight equations and only one parameter, K_R. This over determined problem is solved by a least-squares method. The result depends on the way of defining the eight equations (see details in Appendix-A) and the relative weight of each equation.

In Fig. 4 results of the matching procedure are presented. Two weighting examples are considered: one includes equal weighting for all the eight equations and the other includes zero weighting for the four equations associated with the on-axis response, which means matching only the off-axis response. The matching is done at 29 different frequencies ranging from 0.5 to 10.5 rad/sec, using a logarithmic division of the range. The differences between the two weighting cases (curves c and d of Fig. 4) are apparent only at low and high frequencies (lower than 1 rad/sec and higher than 7 rad/sec). A clear behavior of K_R is noticed: at frequencies lower than 2 rad/sec the optimal K_R obtain values between 2 and 3.5. Between 2 rad/sec and 6 rad/sec, the optimal K_R value is around 1. At frequencies higher than 6 rad/sec, the optimal value of K_R increases rapidly.

The least-squares code is also capable of carrying out a simultaneous least-squares procedure for a few different frequencies. A single least-squares procedure for all the different 29 frequencies (finds the least squares solution for 232 equations, simultaneously) was also performed, for the two weighting examples. The following results were obtained:

- For a least-squares procedure that includes the off-axis and on-axis responses, $K_R = 1.96$.

- For a least-squares procedure that includes only the off-axis responses, $K_R = 1.55$.

The last two results are also presented in Fig. 4 as straight horizontal lines having a constant value of K_R over the entire range (curves a and b). These results of a simultaneous least-squares procedure, present certain "averages" of curves b and c of Fig. 4, and they also agree with the trends of Fig. 3. It is interesting to note that according to the literature the values of K_R that gave good correlation between simulations and flight test results in hover, were K_R = 1.5-1.6. These values agree very well with the present results.

The extended dynamic-inflow model that includes K_R seems to improve the model significantly by adding to it the wake distortion effects. Yet the K_R approach raises two points of concern:

- An accurate solution of the equations that describe the flow through the disk led to the dynamic-inflow equations of Ref. 34. Why this accurate solution does not result in a solution that includes wake distortion effects?

- The dynamic-inflow equations are obtained as a result of solving the momentum equations of an incompressible and inviscid flow. K_R is almost solely calculated using a vortex model. Thus the final model presents a somewhat artificial combination of two different approaches.

Recently, Rosen [Refs. 59-64] presented a new approximate actuator disk model that addresses the above points. The new model was developed using two different approaches:

- An approximate solution of the potential flow equations (incompressible and inviscid flow) through the disk, which is presented in detail in Refs. [59-61]. Small perturbations about a basic state of hover or axial flow are considered. The induced velocity in the basic state includes axial as well as radial components. The equations are developed using a system of coordinates that is attached to the disk. Since the perturbations include axial accelerations as well as pitch and roll rates, this system of coordinates is not an inertial system and the momentum equations should address this fact. During the solution of the equations, a few assumptions and approximations are adopted. The final form includes five equations that describe a linear approximation of the flow through the disk, similar to Eq. 2. These equations include wake distortion effects that are a direct result of Coriolis effects due to the radial induced flow in the basic steady state and the dynamic perturbations (axial motion, pitch rate and roll rate of the disk) about the basic steady state.

- The second approach is based on a vortex theory [Refs. 62-64]. The blades are modeled as lifting lines and the wake includes trailing and shed vortices. By assuming an infinite number of blades, an actuator disk model is

obtained. After adopting certain assumptions and approximations, a system of five ordinary differential equations is obtained that describe a linear distribution of the induced flow through the disk.

Detailed analyses are performed for two "extreme" cases: Hover and a fast axial flow. In the case of a fast axial flow the influence of wake distortion is negligible.

The results of the two approaches for hover, can be described by the following system of equations:

$$\frac{1}{\Omega} m_1 \dot{w}_{zo} + l_1 w_{zo} = \Delta C_T + l_2 w_D \tag{3a}$$

$$\frac{1}{\Omega} [M^1] \begin{Bmatrix} \dot{w}_{zs} \\ \dot{w}_{zc} \end{Bmatrix} + [L^1]^{-1} \begin{Bmatrix} w_{zs} \\ w_{zc} \end{Bmatrix} = \begin{Bmatrix} \Delta C_{LA} \\ \Delta C_{MA} \end{Bmatrix} \tag{3b}$$

$$\frac{1}{\Omega} [M^2] \begin{Bmatrix} \dot{w}_p \\ \dot{w}_q \end{Bmatrix} + [L^2] \begin{Bmatrix} w_p \\ w_q \end{Bmatrix} = \frac{1}{\Omega} \begin{Bmatrix} p_D \\ q_D \end{Bmatrix} \tag{3c}$$

The perturbation of the axial nondimensional induced velocity through the disk, relative to a disk attached system of coordinates, (ν, is:

$$\nu = w_{zo} - w_D + r \left[(w_{zs} + w_p - p_D) \sin\psi + (w_{zc} + w_q - q_D) \cos\psi \right] \tag{4}$$

w_D is the disk nondimensional perturbation in the downward velocity. p_D and q_D are the disk nondimensional perturbations in roll and pitch rates:

$$u_D = w_f - 0.75\dot{\beta}_o / \Omega \tag{5a}$$

$$p_D = p_f - \dot{\beta}_s / \Omega \tag{5b}$$

$$q_D = q_f - \dot{\beta}_c / \Omega \tag{5c}$$

w_f is the perturbation in the fuselage downward velocity. β_o is the rotor conning. m_1, l_1 and l_2 are in general functions of the frequency of the phenomenon, as well as the velocity of the basic flow. The matrices $[M^1]$, $[L^1_H]^{-1}$, $M^2]$ and $[L^2]$ are also functions of the basic flow and the frequency of the perturbations. All the matrices are diagonal and of order 2, where the two terms on the diagonal are identical (pitch and roll are symmetric in an axial flow).

Equation (3c) describes wake distortion effects due to roll and pitch rates of the disk, that result in the induced velocity components w_p and w_q. It is interesting to note that Eq. (3a), for the uniform component of the perturbation in the induced velocity, also includes a wake distortion effect, given by the term l_2 w_D. Equation (3b) is equivalent to the "classical" dynamic-inflow equations for pitch and roll perturbations.

References [60-64] give the various terms for hover and a fast axial flow. Good agreement was shown between the results of the new model and flight test or wind tunnel results. An important point raised in Refs. [59-64] is the fact that the induced velocity is calculated relative to a system of coordinates which is attached to the disk. In many simulation codes the induced velocity relative to an inertial system, which at any moment coincides with the moving system, is used. Then a transformation should be applied where, if (is the induced velocity through the disk relative to an inertial reference system, then:

$$\lambda = \nu + w_{zo} + r (p_D \sin\psi + q_D \cos\psi) \tag{6}$$

Aerodynamic Phase Lag

The approaches of modeling the cross-coupling phenomenon described in the previous two sections, were based on modeling of the physical phenomenon of wake distortion. Another approach is to introduce a correction that fixes the problem without being directly related to a certain physical phenomenon.

The first successful attempt to correct the off-axis prediction, using such an approach, was presented by Tischler et al. [8]. An isolated rotor was tested in a wind tunnel and its responses were compared to a fixed-shaft GenHel model. The presence of the off-axis discrepancy proved that it was solely rotor-related. The discrepancy was successfully corrected after the introduction of an additional swashplate phase angle in GenHel. Tischler et al.[8] summed up the effort by noting that: "the large discrepancy in the coupling responses of GenHel, and the large identified shift of the effective control phasing relative to the actual geometric value used in the wind tunnel test, suggests that a fundamental or first-order phenomenon has been neglected in both the analytical identification structure and GenHel simulation model." Expanding on the findings of Tischler et al., Takahashi et al. [65] and Fletcher [66] implemented an azimuthal rotation in the fixed frame rotor aerodynamics to eliminate the fixed-shaft limitation of the increased swashplate phase angle

approach. This technique was dubbed aerodynamic phase lag (ψ_a). They showed significant improvement in off-axis response agreement between flight test results and calculations of a UH-60.

Mansur and Tischler [57] applied the aerodynamic phase lag technique to a simulation of an AH-64. Results indicated again that significant improvement in the off-axis responses could be achieved in hover. In forward flight, however, the best correlation in the longitudinal and lateral off-axes responses required different values of the phase lag for each axis. This fact is analogous to the different wake distortion coefficients in forward flight, K_p and K_q, as mentioned in the previous Section. However the authors [Ref.57] showed that a compromise value could be selected that result in a good overall improvement.

Successful applications of the aerodynamic phase lag to improve the off-axis response correlation were also reported by Fletcher and Tischler [67] while using the measurements of blade flapping to improve flight mechanics models, and by Tischler [45] while simulating the SBMR wind tunnel tests at $\mu = 0.093$ and 0.233, and by Schulein [68].

Keller and Curtis [23] investigated the possible sources of the model deficiencies that were addressed by the aerodynamic phase lag correction. The study focused on two aspects: the effect of compressibility on the unsteady cross-sectional lift model and the effect of wake distortion due to pitch rate. They continued this investigation also in Ref. [44] and presented the following relation between the aerodynamic phase lag, ψ_a, the wake distortion coefficient, K_p, and unsteady aerodynamics:

$$\psi_a = \tan^{-1}(\tan\psi_{au} + \gamma K_p / 16) \tag{7}$$

ψ_{au} is the phase lag due to unsteady aerodynamics alone, including compressibility effects. γ is the rotor Lock number. It should be emphasized that Eq. (7) is based on various assumptions, including steady-pitch or roll.

Equation (7) clearly indicates that the aerodynamic phase lag correction does not have a direct physical basis as the wake distortion coefficient. ψ_a depends on γ, which is not a function of aerodynamic characteristics alone, but presents a ratio between aerodynamic and inertial effects. Thus the aerodynamic phase lag becomes also a function of inertia effects. This aspect will be studied in Section - Influence of the number of blades.

Probably the best way to look at ψ_a, is as a correction that accounts for various effects that may include wake distortion and unsteady cross-sectional aerodynamics, but may also account for: blade torsional and bending flexibilities, fuselage aerodynamic interference effects, as well as other phenomena that are not otherwise properly modeled.

The resulting total aerodynamic phase lag is implemented in time-history simulations via a first-order filter, applied to the rotating frame aerodynamic components:

$$F(s) = \frac{1}{\tau_s s + 1} \tag{8}$$

where

$$\tau_a = \frac{1}{\Omega}\tan\psi_a \tag{9}$$

Essentially, the instantaneous lift and drag coefficients for each blade-element, in the rotating frame, are processed through the first-order lag of Eq. (8) before they are used to calculate the elemental forces and moments.

Numerical perturbation models are treated differently than time-history models. If the aerodynamic phase lag filter of Eq. (8) was applied at the rotating frame blade element level, it would essentially add one state for each aerodynamic load component at every blade element and the resulting model would have far too many states. A much simpler but sufficiently accurate alternative approach was adopted and validated in which the aerodynamic lag was applied to the summed first harmonic components of the six aerodynamic forces and moments in the fixed frame, thus adding only six aerodynamic states. For example, the equations for the "lagged" aerodynamic pitch and roll moments (M_{lc}', M_{ls}') in terms of the unlagged moments (M_{lc}, M_{ls}), are given by [Ref. 23]:

$$\begin{aligned}\tau_a \dot{M}_{lc}' &= -\tau_a \Omega \dot{M}_{ls}' - M_{lc}' + M_{lc} \\ \tau_a \dot{M}_{ls}' &= -\tau_a \Omega \dot{M}_{lc}' - M_{ls}' + M_{ls}\end{aligned} \tag{10}$$

This calculation is made at each azimuth in the linearization scheme. The approximation introduced by applying the phase lag correction at the fixed-frame level, as compared to the blade-element level, was found to be very accurate.

Research carried out at Ames Research Center has identified optimal aerodynamic phase lag values for various helicopter models. Collecting this information is important if aerodynamic phase lag is to be used in situations where flight data is unavailable. A "carpet plot" of ψ_a as a function of key configuration parameters will allow the method to be used for simulations of new helicopter designs, and in other situations where identifying aerodynamic phase lag from flight data is impossible. A summary of findings is presented in Table-1.

In a later investigation Schulein et al. [69] used a special code to investigate the trends of at three forward airspeeds. The results are shown in Fig. 5.

In Figs. 6a,b the frequency response of a hovering UH-60 using five different values of the aerodynamic phase lag, are presented: 0° (no correction), 35°, 40°, 45° and 50°. Figure 3a shows that, similar to the case of K_R, the influence of the phase lag on the on-axis response is mainly limited to low and high frequencies. At low frequencies there is in general an improvement in the agreement, with flight test results, of amplitude and phase, when the aerodynamic phase lag is applied. There is also an improvement in the agreement of amplitude and phase of (q_f/lon) at high frequencies. A significant improvement is shown in the off-axis response in Fig. 6b. The difference of 360° in phase of (p_f/lon), for frequencies higher than 3 rad/sec, was discussed in relation to Fig. 3b. Overall an aerodynamic phase lag of 45° gives a good agreement between the simulation results and flight test results for hover. This value agrees very well with the results of Table-1.

Similar to the case of the K_R correction in the previous Section, also here a least-squares procedure is used to find the optimal aerodynamic phase lag for the four cases shown in Fig.4. The results are shown in Fig.7.

The results in Fig.7 are very similar in nature to the results of Fig. 4. In the case of applying a single least-squares procedure at each frequency; values of phase lag over 47° are obtained for frequencies lower than 2 rad/sec. As in Fig. 4 the analysis that includes also the on-axis response equations, gives lower values. For frequencies in the range 2-6 rad/sec, lower values of the phase lag, in the vicinity of 20°, are obtained. For frequencies higher than 6 rad/sec the phase lag values increase, but there is a difference between the behavior in Figs. 4 and 7 in this region. If a simultaneous least-squares procedure is performed, for all the 29 frequencies in the entire range, practically identical values are obtained for both examples (curves a and b), giving a value of 45.4°.

Discussion

Summary of the Previous Results

Figures 8a,b present a summary of the results for the frequency response of a UH-60 in hover. In addition to the flight test results the following simulation results are shown:

- A complete model of TEMURA.
- A dynamic-inflow model with a K_R correction, where K_R = 1.96 (the result of a simultaneous least-squares procedure in Section - Actuator Disk Models).
- A dynamic-inflow model with an aerodynamic phase lag of ψ_a = 45.4° (the result of a simultaneous least-squares procedure in Section - Aerodynamic Phase Lag).
- Results of the new actuator disk model of Refs. 59-64.

In general the results of all the simulations are similar.

In the case of the on-axis response, Fig. 8a, TEMURA gives a very good agreement with the amplitude throughout the entire range of frequencies. The other models predict somewhat higher amplitudes at low frequencies. Concerning the phase angle of the on-axis response, TEMURA predicts somewhat higher angles (+25°) at low frequencies, while the corrections, including K_R and ψ_a, exhibit better agreement with the flight test results. At high frequencies TEMURA and the ψ_a correction give higher phase angles, while the correction and the new model show nice agreement with the flight test results.

Concerning the phase angle of the off-axis response, Fig. 8b, in general the agreement of all the simulations with the flight test results is good. In the case of (p_f/lon) the K_R and ψ_a corrections exhibit a different trend in the region 1-3 rad/sec, that was discussed in relation to Fig. 3b, while TEMURA and the new model exhibit the same trend as shown by the flight test results. A similar problem is also shown in the results of the ψ_a correction in the region 6-8 rad/sec.

The amplitudes of the simulations of (q_f/lat) exhibit certain differences at frequencies lower than 1 rad/sec. In

the range 1-5 rad/sec there is a fairly good agreement between the different simulations and flight test results. At higher frequencies differences appear again.

In the case of the amplitude of (p_f/lon), all simulations predict the minimum at 2-2.3 rad/sec, but the amplitude of this minimum varies. There are also other differences in the amplitudes between the simulations, at different frequencies: The new model shows good agreement with TEMURA, the K_R and ψ_a corrections exhibit better agreement with the flight test results at low frequencies, and worse agreement (than TEMURA) at high frequencies.

It can be concluded at this point, based on the comparisons between the simulation results and the flight test results, that TEMURA and the correction methods using K_R or ψ_a that have been obtained by a least-squares procedure of matching to the results of TEMURA, have been verified.

As already indicated above, various researchers pointed out, that the values of the corrections, either K_R or ψ_a, may depend on: flight speed, blade flapping frequency (otherwise offset) and thrust. These issues will be studied in what follows. In all the cases the UH-60 in hover (and its rotor) will be used to study the influence of the various effects.

Investigation of Eq.(7)

As indicated above, the wake distortion coefficient, K_R, and the aerodynamic phase lag, ψ_a, present two different approaches of correcting the dynamic-inflow model for missing effects, mainly the wake distortion effect. Equation (7) connects K_R and ψ_a. This equation, presented in Ref. [23], which is based on certain assumptions and simplifications, will be investigated in the same section.

TEMURA includes a detailed model of the cross-sectional unsteady aerodynamics, including compressibility effects. Although compressibility may have a significant influence in certain cases [see Ref. 22], especially problems of rotor dynamics and aeroelasticity, studies using TEMURA have shown that compressibility influences on flight mechanics are small and may be neglected. These results agree with those of other researchers [for example Refs.25 or 47] that concluded that the influence of unsteady (cross-sectional) aerodynamic effects on flight mechanics is very small. Thus ψ_{au} in Eq. (7) will be neglected. Then Eq. (7) reduces to:

$$\psi_a \equiv tg^{-1}\ (\gamma K_R / 16) \tag{11}$$

For the UH-60 one obtains:

$$\psi_a \equiv tg^{-1}\ (K_R / 2) \tag{12}$$

As indicated above, while discussing Fig.4, at frequencies lower than 2 rad/sec K_R varies between 2 and 3.5. According to Eq. (12) this means ψ_a values between 45° and 60°. In Fig. 7, ψ_a for frequencies lower than 2 rad/sec, varies between 47° and 67°. In the medium range of frequencies, 2-6 rad/sec, K_R is close to 1. This value corresponds, according to Eq. (12), to ψ_a = 26°. In Fig. 7 the values of ψ_a in this region are usually slightly over 20°. At high frequencies, over 6 rad/sec, the behavior of K_R and ψ_a vary significantly (although on the average they both exhibit an increase in their values). As indicated above Eq. (7) is based on the assumption of a steady pitch or roll, and thus there may be problems in applying it at high frequencies.

The above results indicate that Eq. (7) may be correct for low frequencies, but it ceases to hold at high frequencies.

When it comes to finding average representative values of K_R and ψ_a, for the entire range of frequencies (0.5-10.5 rad/sec), by using a simultaneous least-squares procedure, then using Eq. (12) seems more problematic. The values of K_R = 1.54 and K_R = 1.96 give values of ψ_a = 37.6° and ψ_a = 44.4°, respectively, compared to the value of ψ_a = 45.4° for both cases, as presented in Fig. 7. This problem may result from the influence of high frequencies, which, as indicated above, exhibit significant differences between both cases. The results in the next sub-sections will further show that there are basic differences between K_R and ψ_a corrections and thus it seems problematic to try and use simple relations between these two different approaches.

Influence of Flapping Frequency

The nondimensional basic flapping frequency (the dimensional frequency is divided by (Ω), ω_β, of a UH-60, is 1.036. This frequency was varied by changing the offset of the blade (the original offset, divided by radius, is 0.047). At each offset, the optimal values of K_R and ψ_a were calculated by applying the simultaneous least-squares procedure on 29 frequencies in the range 1-10

rad/sec. This is the range of frequencies which is important for flight mechanics and handling-qualities applications. In all the cases the four response variables (two on-axis and two off-axis) have the same weighting. In addition the weighting between amplitude and phase angles is chosen as 7.57 degree/dB. This ratio is universally used in the handling-qualities system identification community.

In Fig. 9 the optimal values of K_R are presented. It is clearly shown that K_R increases with the flapping frequency, from a value of slightly less than 1.5 for $\omega_\beta = 1.0$, to a value slightly over 2.0 for $\omega_\beta = 1.1$. The increase is sharper at low flapping frequencies, while at higher flapping frequencies the value is practically constant.

In Fig.10 the optimal aerodynamic phase lag angle, ψ_a, is shown. This angle decreases with the flapping frequency from a value of 50° for an articulated rotor, to a value of 40° for a "rigid" rotor. Similar to the case of, K_R, the decrease is sharper at low flapping frequencies, while at high frequencies the value is practically constant. There is a relatively large decrease at value of $\omega_\beta \approx 1.05$-$1.06$.

Influence of Thrust Coefficient

The thrust coefficient of the "nominal" UH-60 is 0.00536. The thrust coefficient was varied in the range 0.00058-0.0133, and at different values of the thrust coefficient the optimal K_R and ψ_a values, were calculated (range of frequencies 1-10 rad/sec, 29 different values).

The results for K_R are shown in Fig.11. The values vary between $K_R = 1.5$ and $K_R = 2.3$. Thus taking a representative value of $K_R = 1.9$ seems appropriate. This value, again, agrees with the values that have been used in the literature in successful simulations.

The optimal values for ψ_a are shown in Fig.12. At the lowest C_T, $\psi_a = 40°$. It increases to 45.4° at the nominal C_T value, and approaches a value of 50° for high thrust coefficients.

Influence of the Number of Blades

The number of blades was varied between 1 and 6. The chord was also varied such that the solidity remained constant and equal to the nominal value. Also the thrust coefficient remained unchanged.

K_R and ψ_a were calculated in the same manner as in the previous figures.

Figure 13 shows that K_R drops from a value of 2.3 for two blades, to a value of 1.8 for six blades.

The optimal ψ_a values are shown in Fig.14. The aerodynamic phase lag drops from 50° for two blades to 44° for six blades.

Conclusions on the Variations of K_R and ψ_a

For all the cases that were considered, K_R varies between 1.5 and 2.2. The aerodynamic phase lag changes in the range 40°-50°. Values of $K_R = 2$ and $\psi_a = 45°$ seem to be representative of typical rotors at hover.

Conclusions

Until recently the prediction of the cross-coupling (off-axis) behavior of helicopters and helicopter rotors was beyond the capability of all the simulation codes. Although the off-axis response is sensitive to various effects like: blade flexibility, aerodynamic interference with the fuselage and others, it became clear that the wake distortion phenomenon, which was missing from all the simulations, is the prime contributor to the off-axis response.

Detailed models of the wake distortion effect have been developed. These include prescribed wake and the more sophisticated free wake models. The models are fairly complicated and require large computer resources and long computing times. This makes these models inappropriate for various applications like flight mechanics simulations, especially real time simulations. For such purposes two simplified approximate descriptions of the wake distortion phenomena have been used:

- Adding the wake distortion coefficient to the regular dynamic-inflow equations. A single coefficient is used for the axisymmetric case of hover or axial flight, K_R. For the asymmetric case of forward flight two different coefficients are used: K_p and K_q.
- Adding an aerodynamic phase lag, ψ_a, to a regular dynamic-inflow model.

The K_R correction presents an approximate simplified description of the phenomenon of wake distortion. The approximation involves, for example, the assumption of

steady pitch or roll, without considering transient effects. Another approximation is the separate calculation of the wake distortion effect using a vortex model, and then adding it, in a simple quasi-algebraic manner, to a dynamic-inflow model that has been developed using a completely different approach.

The aerodynamic phase angle, ψ_a, is a correction method that is "equivalent", in its effect on the helicopter response, to the wake distortion. The aerodynamic phase lag is not a physical description, even approximate, of the phenomenon.

It was pointed out in the literature, and shown clearly above, that the optimal correction of the dynamic-inflow model, for wake distortion effects, either by using K_R or ψ_a, is a function of the flight speed and the frequency of the perturbation. Yet it is often possible to use an average representative value for a certain flight speed.

In addition to their dependence on the speed of flight and frequency, K_R or ψ_a depend, in general, on: the rotor flapping frequency, the thrust coefficient and number of blades. Yet it is possible to choose representative values of K_R or ψ_a for a certain flight speed that will give good results for a wide range of parameters.

By using a detailed code like TEMURA, and matching between its results and ψ_a or K_R corrections, with the help of a least-squares procedure (or any other equivalent procedure), it is possible to obtain the right ψ_a or K_R corrections for new designs.

Recently, a new approximate actuator disk model of a rotor in hover or axial flow has been developed. This model is much simpler than the detailed free or prescribed wake models and requires much less computer resources. On the other hand, it includes many elements that are missing from ψ_a or K_R corrections. It is based on a unified approach where the wake distortion effects are obtained as an integral part of a consistent derivation of the entire model. In fact, two approaches, a vortex model and an approximate solution of the potential flow equations of an incompressible inviscid flow, give the same model. The new model includes a dynamic transient behavior of the wake distortion effects, which may be important in the modeling of real maneuvers.

Most of the results, which were reviewed and presented above, deal with hover. Indeed most of the research concentrated on hover because the cross-coupling effects are strong in this flight condition and tend to disappear in forward flight. The hover case, with its axisymmetry, also offers some advantages in analytical or numerical derivations. Studies that dealt with forward flight indicated that at small advance ratios there may be interesting phenomena associated with the wake distortion effects. According to those studies the intensity of the wake distortion at low advance ratios might even exceed the intensity of the effect in hover. Moreover, the wake distortion effects may be smaller at forward flight, but not necessarily negligible and sometimes even important. Therefore in the coming years extensions of the various models to forward flight, and analysis of the various effects as functions of the advance ratio, will be required.

Every model has to be verified. More flight test results of different helicopters - having different flapping frequencies, different thrust coefficients and different number of blades - flying at various speeds, are needed in order to verify the newly developed models. Moreover, tests of isolated rotors in a wind tunnel offer means of separating between the main aerodynamic phenomena associated with the rotor, and the coupling of those phenomena with the fuselage dynamics and aerodynamics. Therefore controlled wind-tunnel tests of isolated rotors may offer very valuable data for verifying the models.

Acknowledgement

The research that led to this review was carried out during the last few years under the US/Israel MOA on "Rotorcraft Aeromechanics and Man-Machine Integration Technology".

References

1. Prouty, R.W., "The Case of the Cross-Coupling Mystery", Rotor and Wing, Vol.28, No.6, 1994, pp.48-49.

2. Eshow, M.M., Oriandi, D., Bonaila, B. and Barbieri, S., "Results of an A-109 Simulation Validation and Handling Qualities Study", Fourteenth European Rotorcraft Forum, Milano, Italy, 20-23 September 1988, Paper No. 64.

3. Harding, J.W. and Bass, S.M., "Validation of a Flight Simulation Model of the AH-64 Apache Attack Helicopter Against Flight Test Data", Proceedings of the 46th Annual Forum of the American Helicopter Society, Washington D.C, May 1990, pp. 1309-1325.

4. Ballin, M.G. and Dalang-Secrtan, M.A., "Validation of the Dynamic Response of a Blade-Element UH-60 Simulation Model in Hovering Flight", J. of the American Helicopter Society, Vol.36, No.4, 1991, pp. 77-88. (Condensed version of a paper presented at the 46th Annual Forum of the AHS, Washington D.C., May 1990).

5. Chaimovich, M., Rosen, A., Rand, O., Mansur, M.H. and Tischler, M.B., "Investigation of the Flight Mechanics Simulation of a Hovering Helicopter", Proceedings of the American Helicopter Society 48th Annual Forum, Washington D.C, June 3-5, 1992, pp. 1237-1256.

6. Curtiss, H.C., "On the Calculation of the Response of Helicopters to Control Inputs", Proceedings of the 18th European Rotorcraft Forum, Avignon, France, September 14-17, 1992, paper no. F07.

7. Fletcher, J.W., "Identification of UH-60 Stability Derivative Models in Hover from Flight Test Data", Proceedings of the American Helicopter Society 49th Annual Forum, St. Louis, Missouri, May 19-21, 1993, pp.183-210.

8. Tischler, M.B., Drissoll, J.T., Cauffman, M.G. and Freedman, C.J., "Study of Bearingless Main Rotor Dynamics from Frequency-Response Wind Tunnel Test Data", Proceedings of the American Helicopter Society Aeromechanics Specialists Conference, San Francisco, CA, January 19-21, 1994, pp. 6.3-1-6.3-26.

9. He, C. and Lewis, W.D., "A Parametric Study of Real Time Mathematical Modeling Incorporating Dynamic Wake and Elastic Blades", Proceedings of the 48th Annual Forum of the American Helicopter Society, Washington, D.C, June 3-5, 1992, pp.1181-1196.

10. Sturisky, S.H. and Schrage, D.P., "System Identification Validation of an AH-64 Aeroelastic Simulation Model", Proceedings of the American Helicopter Society 49th Annual Forum, St. Louis, Missouri, May 19-21, 1993, pp. 481-504.

11. Turnour, S.R. and Celi, R., "Effects of Blade Flexibility on Helicopter Stability and Frequency Response", Proceedings of the 19th European Rotorcraft Forum, Cernobbio, Italy, September 1993, pp.(H3-1) - (H3-22).

12. Grnhagen, W., "Dynamic Inflow Modeling for Helicopter Rotors and Its Influence on the Prediction of Cross-Coupling", Proceedings of the American Helicopter Society Aeromechanics Specialist Conference, Fairfield, CT, October 11-13, 1995, pp. (4-1) - (4-10).

13. Isser, A. and Rosen, A., "A Model of the Unsteady Aerodynamics of a Hovering Helicopter Rotor that Includes Variations of the Wake Geometry", J. of the American Helicopter Society, Vol. 40, No. 3, 1995, pp. 6-16 (also Proceedings of the 34th Israel Annual Conference on Aerospace Sciences, February 1994, pp. 90-105).

14. Rosen, A. and Isser, A., "Investigation of the Technion Model of Unsteady Rotor Aerodynamics (TEMURA)", Presented at the Sixth International Workshop on Dynamics and Aeroelastic Stability Modeling of Rotorcraft Systems, University of California, Los Angeles (UCLA), November 8-10, 1995.

15. Rosen, A., Isser, A. and Yoshpe, M., "The Influence of Unsteady Aerodynamics and Inter-Blade Aerodynamic Coupling on the Blades Response to Harmonic Variations of Their Pitch Angles", The Aeronautical Journal, Vol. 100, No. 991, 1996, pp. 27-35.

16. Rosen, A. and Isser, A., "The Influence of Unsteady Aerodynamic Effects on the Coupled Free Vibrations of Rotor Flapping and Body Pitch and Roll in Hover", J. of the American Helicopter Society, Vol. 41, No.3, 1996, pp.208-218.

17. Rosen, A. and Isser, A., "A New Model of Rotor Dynamics During Pitch and Roll of a Hovering Helicopter", J. of the American Helicopter Society, Vol. 40, No. 3, 1995, pp. 17-2 (also Proceedings of the 50th Annual Forum of the American Helicopter Society, Washington D.C, May 11-13, 1994, pp. 409-426).

18. Takasawa, K., "On the Pitch Damping Moment in Hovering of a Rigid Helicopter Rotor", NASA TT F-15,010, September 1973, 140 pp.

19. Takasawa, K., "On the Aerodynamic Damping Moment in Pitch of a Rigid Helicopter Rotor in Hovering. Part I. Experimental Phase", Transactions of the Japan Society for Aeronautical and Space Sciences, Vol.16, No.31, 1973, pp.19-36.

20. Takasawa, K., "On the Aerodynamic Damping Moment in Pitch of a Rigid Helicopter Rotor in Hovering. Part II. Analytical Phase", Transactions of the Japan Society for Aeronautical and Space Sciences, Vol. 16, No. 32, 1973, pp. 77-101.

21. Isser, A. and Rosen, A., "The Pitch Damping of a Hovering Rigid Rotor ", J. of the American Helicopter Society, Vol.42, No.1, 1997, pp.96-99.

22. Rosen, A. and Yaffe, R., "Compressibility Effects on the Unsteady Aerodynamics of a Rotor in Hover or Axial Flight", J. of the American Helicopter Society, Vol.46, No.1, 2001, pp.44-58.

23. Keller, J.D. and Curtiss, H.C., "Modeling the Induced Velocity of a Maneuvering Helicopter", Proceedings of the 52nd Annual Forum of the American Helicopter Society, Washington D.C, June 4-6, 1996, pp. 841-851.

24. Bagai, A., Leishman, J.G. and Park, J., "Aerodynamic Analysis of a Helicopter in Steady Maneuvering Flight Using a Free-Vortex Rotor Wake Model", J. of the American Helicopter Society, Vol. 44, No. 2, 1999, pp. 109-120. (A revised version of a paper presented at the AHS Technical Specialists' Meeting on Rotorcraft Acoustics and Aerodynamics, Williamsburg, VA, October 1997).

25. Park, J.S. and Leishman, J.G., "Investigation of Unsteady Aerodynamics on Rotor Wake Effects in Maneuvering Flight", Proceedings of the 55th Annual Forum of the American Helicopter Society, Montreal, Canada, May 1999, pp. 467-480.

26. Leishman, J.G., Bhagwat, M.J. and Bagai, A., "Free-Vortex Filament Methods for the Analysis of Helicopter Rotor Wakes", J. of Aircraft, Vol. 39, No. 5, 2002, pp. 759-775.

27. Theodore, C.R. and Celi, R., "Helicopter Flight Dynamic Simulation with Refined Aerodynamics and Flexible Blade Modeling", J. of Aircraft, Vol. 39, No. 4, 2002 (also Proceedings of the 56th Annual Forum of the American Helicopter Society, Virginia Beach, Virginia, May 2000, pp. 857-872).

28. Bhagwat, M.J. and Leishman, J.G., "Rotor Aerodynamics During Maneuvering Flight Using a Time-Accurate Free-Vortex Wake", J. of the American Helicopter Society, Vol. 48, No. 3, 2003, pp. 143-158 (also Proceedings of the 57th Annual Forum of the American Helicopter Society, Washington, DC, May 9-11, 2001).

29. Ananthan, S. and Leishman, J.G., "Transient Helicopter Rotor Wakes in Response to Time-Dependent Blade Pitch Inputs", J. of Aircraft, Vol. 41, No. 5, 2004, pp. 1025-1041 (also Proceedings of the 59th Annual Forum of the American Helicopter Society, Phoenix, AZ, May 6-8, 2003, pp. 1741-1762).

30. Ananthan, S. and Leishman, J.G., "Helicopter Rotor Wake Dynamics During Simulated Tactical Maneuvers", Proceedings of the 60th Annual Forum of the American Helicopter Society, Baltimore, MD, June 7-10, 2004, pp. 949-980.

31. Basset, P.M., "Modeling of the Dynamic Inflow on the Main Rotor and the Tail Components in Helicopter Flight Mechanics", Proceedings of the 22nd European Rotorcraft Forum, Brighton, UK, September 17-19, 1996 (also Proceedings of the 53rd Annual Forum of the American Helicopter Society, Vol. 2, 1997, pp. 1643-1656).

32. Basset, P. M. and Tchen-Fo, F., "Study of the Rotor Wake Distortion Effects on the Helicopter Pitch-Roll Cross-Couplings", 24th European Rotorcraft Forum, Marseilles, France, September 1998, FMO6.1-FMO6.13.

33. Graham, Jr. K.S. and Katz, A., "Vortex Generated Rotor Wake Model for Real Time Simulation", Proceedings of the 56th Annual Forum of the American Helicopter Society, Virginia Beach, Virginia, May 2-4, 2000, pp. 556-568.

34. Pitt, D.M. and Peters, D.A., "Theoretical Prediction of Dynamic-Inflow Derivatives", Vertica, Vol.5, 1981, pp. 21-34.

35. Peters, D.A. and He, C.J., "A Closed-Form Aerodynamic Theory for Lifting Rotors in Hover and Forward Flight", Proceedings of the 43rd Annual Forum

of the American Helicopter Society, St. Louis, Missouri, May 18-20, 1987, pp. 839-865.

36. Keller, J.D., "An Investigation of Helicopter Dynamic Coupling Using an Analytical Model", J. of the American Helicopter Society, Vol. 41, No. 4, 1996, pp. 322-330. (Also Proceedings of the 21st European Rotorcraft Forum, St. Petersburg, Russia, August 1995).

37. Arnold, U.T.P., Keller, J.D., Curtiss, H.C. and Reichert, G., "The Effect of Inflow Models on the Predicted Response of Helicopters", J. of the American Helicopter Society, Vol. 43, No. 1, 1998, pp. 25-36 (also Proceedings of the 21st European Rotorcraft Forum, St. Petersburg, Russia, August 1995).

38. Krothapalli, K.R., Prasad, J.V.R. and Peters, D.A., "Development of a Comprehensive Wake Theory for Lifting Rotors", AIAA Atmospheric Flight Mechanics Conference, San Diego, CA, July 1996, AIAA-96-3390, pp. 767-772.

39. Barocela, E., Peters, D.A., Krothapalli, K.R. and Prasad, J.V.R., "The Effect of Wake Distortion on Rotor Inflow Gradients and Off-Axis Coupling", AIAA Atmospheric Flight Mechanics Conference, New Orleans, LA, August 1997, AIAA-97-3579, pp. 272-282.

40. Krothapalli, K.R., Prasad, J.V.R. and Peters, D.A., "A Generalized Dynamic Wake Model with Wake Distortion", Proceedings of the 54th Annual Forum and Technology Display of the American Helicopter Society, Washington D.C, May 1998, pp. 527-536.

41. Krothapalli, K.R., Prasad, J.V.R. and Peters, D.A., "Helicopter Rotor Dynamic Inflow Modeling for Maneuvering Flight", J. of the American Helicopter Society, Vol. 46, No. 2, 2001, pp. 129-138 (also Proceedings of the 55th Annual Forum of the American Helicopter Society, Montreal, Canada, May 1999, pp. 498-510).

42. Peters, D.A., Morillo, J.A. and Nelson, A.M., "New Developments in Dynamic Wake Modeling for Dynamics Applications", J. of the American Helicopter Society, Vol. 48, No. 3, 2003, pp. 120-127 (also Proceedings of the 57th Annual Forum of the American Helicopter Society, Washington D.C, May 9-11, 2001, pp. 1150-1159).

43. Prasad, J.V.R., Fanciullo, T., Zhao, J. and Peters, D.A., "Towards a High Fidelity Rotor Inflow Model for Maneuvering and In-Ground Effect Flight Simulation", Proceedings of the 57th Annual Forum of the American Helicopter Society, Washington D.C, May 9-11, 2001, pp. 1176-1186.

44. Keller, J.D. and Curtiss, H.C., "A Critical Examination of the Methods to Improve the Off-Axis Response Prediction of Helicopters", Proceedings of the 54th Annual Forum of the American Helicopter Society, Washington D.C., May 1998, pp. 1134-1147.

45. Tischler, M.B., "Identification of Bearingless Main Rotor Dynamic Characteristics from Frequency-Response Wind-Tunnel Test Data", J. of the American Helicopter Society, Vol. 44, No.1, 1999, pp. 63-76.

46. Hammers, M. and von Grnhagen, W., "Nonlinear Helicopter Model Validation Applied to Real Time Simulations", Proceedings of the 53rd Annual Forum of the American Helicopter Society, Virginia Beach, Virginia, April 29 - May 1, 1997, pp. 958-972.

47. He, Chengjian, He, C.S. and Chen, Weibin, "Rotorcraft Simulation Model Enhancement to Support Design, Testing and Operational Analysis", J. of the American Helicopter Society, Vol. 45, No. 4, 2000, pp. 284-292 (also Proceedings of the 55th Annual Forum of the American Helicopter Society, Montreal, Canada, May 1999, pp. 2122-2139).

48. Turnour, S.R. and Celi, R., "Effects of Unsteady Aerodynamics on the Flight Dynamics of an Articulated Rotor Helicopter", AIAA J. of Aircraft, Vol. 34, No. 2, 1997, pp. 187-196.

49. Tchen-Fo, F., Eglin, P., Gimoret, B., Desoper, A., Hellard, S., von Grnhagen, W. and Roth, G., "Comparison between Experimental and Predicted Isolated Helicopter Rotor Transfer Functions for Unsteady Inputs on the Controls", Proceedings of the 56th Annual Forum of the American Helicopter Society, Virginia Beach, Virginia, May 2000, pp. 911-927.

50. Hamers, M. and Basset, P.M., "Application of the Finite State Unsteady Wake Model in Helicopter Flight Dynamic Simulation", Proceedings of the 26th European Rotorcraft Forum, The Hague, The Netherlands, September 2000, pp. 27.1-27.16.

51. Smith, S.J., "Helicopter Simulation Modeling Techniques for Meeting FAA AC120-63 Level D Qualification Requirements", Proceedings of the 56th Annual Forum of the American Helicopter Society, Virginia Beach, Virginia, May 2-4, 2000, pp. 1101-1109.

52. Krmer, P., Gimonet, B. and von Grnhagen, W., "A Systematic Approach to Nonlinear Rotorcraft Model Indentification", Aerospace Science and Technology, Vol. 6, 2002, pp. 579-590.

53. Jategaonkar, R., Fischenberg, D. and von Gruenhagen, W., "Aerodynamic Modeling and System Identification from Flight Data-Recent Applications at DLR", J. of Aircraft, Vol. 41, No. 4, 2004, pp. 681-691.

54. Zhao, J., Prasad, J.V.R. and Peters, D.A., "Rotor Dynamic Wake Distortion Model for Helicopter Maneuvering Flight", Proceedings of the 58th Annual Forum of the American Helicopter Society, Montreal, Canada, 2002, pp. 2370-2380.

55. Zhao, J., Prasad, J.V.R. and Peters, D.A., "Investigation of Wake Curvature Dynamics for Helicopter Maneuvering Flight Simulation", Proceedings of the American Helicopter Society 59th Annual Forum, Phoenix, Arizona, May 6-8, 2003, pp. 1887-1901.

56. Zhao, J., Prasad, J.V.R. and Peters, D.A., "Validation of a Rotor Dynamic Wake Distortion Model for Helicopter Maneuvering Flight Simulation", Proceedings of the American Helicopter Society 60th Annual Forum, Baltimore, Maryland, June 7-10, 2004, pp. 331-348.

57. Mansur, M.H. and Tischler, M.B., "An Empirical Correction for Improving Off-Axis Response in Flight Mechanics Helicopter Models", J. of the American Helicopter Society, Vol. 43, No. 2, 1998, pp. 94-102 (also Proceedings of the AGARD Flight Vehicle Integration Panel Symposium on "Advances in Rotorcraft Technology", Ottawa, Canada, May 27-30, 1996, A22-1-10).

58. Curtiss, H.C., "Aerodynamic Models and the Off-Axis Response", Proceedings of the 55th Annual Forum of the American Helicopter Society, Montreal, Canada, May 1999, pp. 2037-2040.

59. Rosen, A., "Approximate Actuator Disk Model of a Rotor During Hover or Axial Flight", Proceedings of the 41st Israel Annual Conference on Aerospace Sciences, February 21-22, 2001, pp. 284-299.

60. Rosen, A., "Results of a New Approximate Actuator Disk Model of a Rotor in Pitch and Roll", Proceedings of the 27th European Rotorcraft Forum, Moscow, September 2001, pp. 67-1-67-12.

61. Rosen, A., "Approximate Actuator Disk Model of a Rotor in Hover or Axial Flow Based on Potential Flow Equations", J. of American Helicopter Society, Vol. 49, No. 1, 2004, pp. 80-92.

62. Rosen, A., "Approximate Actuator Disk Model of a Rotor During Hover or Axial Flow", Faculty of Aerospace Engineering, Technion-Israel Institute of Technology, Haifa, Israel, TAE No. 873, June 2001.

63. Rosen, A., "Approximate Actuator Disk Model of a Rotor", Proceedings of the American Helicopter Society Aerodynamics, Acoustics and Test and Evaluation Technical Specialists Meeting, San Francisco, CA, January 23-25, 2002.

64. Rosen, A., "Approximate Actuator Disk Model of Rotor in Hover or Axial Flow Based on Vortex Modeling", J. of the American Helicopter Society, Vol. 49, No. 1, 2004, pp. 66-79.

65. Takahashi, M.D., Fletcher, J.W. and Tischler, M.B., "Development of a Model Following Control Law for In-flight Simulation Using Analytical and Identified Models", Proceedings of the 51st Annual Forum of the American Helicopter Society, Fort Worth, TX, May 1995, pp. 343-356.

66. Fletcher, J.W., "Identification of Linear Models of the UH-60 in Hover and Forward Flight", Proceedings of the 21st European Rotorcraft Forum, St. Petersburg, Russia, 29 August - 1 September, 1995, pp. VII-4-1,14.

67. Fletcher, J.W. and Tischler, M.B., "Improving Helicopter Flight Mechanics Models with Laser Measurements of Blade Flapping", Proceedings of the 53rd Annual Forum of the American Helicopter Society, Virginia Beach, Virginia, April 29 - May 1, 1997, pp. 1467-1494.

68. Schulein, G.J., "Improvements to a High Fidelity Helicopter Math Model", M.Sc. Thesis, Department of Mechanical and Aeronautical Engineering, University of California, Davis, CA, June 2001.

69. Schulein, G.J., Tischler, M.B., Mansur, M.H. and Rosen, A., "Validation of Cross-Coupling Modeling Improvements for UH-60 Flight Mechanics Simulations", J. of the American Helicopter Society, Vol.47, No. 3, 2002, pp. 209-213.

70. Levenberg, K., "A Method for the Solution of Certain Problems in Least Squares", Quarterly of Applied Mathematics, Vol.2, 1944, pp. 164-168.

71. Marquardt, D., "An Algorithm for Least-Squares Estimation of Nonlinear Parameters", SIAM J. on Applied Mathematics, Vol.11, 1963, pp. 431-441.

Appendix-A

Least-Squares Method to Calculate the Optimal Corrections

As indicated in the text, two parameters are used to correct the helicopter response:

1. The wake distortion coefficient, K_R.
2. The aerodynamic phase lag, ψ_a.

These corrections are used separately (either $K_R \neq 0$ and $\psi_a = 0$, or $K_R = 0$ and $\psi_a \neq 0$), although the procedure can also be carried out for both of them simultaneously ($K_R \neq 0$ and $\psi_a \neq 0$).

The main goal is correcting the off-axis response, namely (q_f/lat) and (p_f/lon), without deterioration in the good agreement of the on-axis response: (q_f/lon) and (p_f/lat). Each of these variables is described in TEMURA by a complex number, representing amplitude and phase. It is desired to match both of them.

Let us concentrate on a representative response parameter, its real part will be denoted $\overline{R}$ and its imaginary part is $\overline{I}$. If $\overline{R}$ and $\overline{I}$ are obtained by TEMURA (the complete model), then they are denoted $\overline{R}_{us}$ and $\overline{I}_{us}$. If a corrected dynamic-inflow model is used, then these parts are denoted $\overline{R}_{di}$ and $\overline{I}_{d}$i. K_R or ψ_a should be chosen in such a way that the differences between the results of TEMURA and the corrected dynamic-inflow model, will be minimal. This can be achieved by matching the real and imaginary parts of both, but in doing that the physical meaning is lost since the real and imaginary parts by themselves do not have clear physical meaning. Investigations have shown that it is preferable to match separately the amplitude and phase angle of both.

Matching the amplitude is equivalent to satisfying the following expression:

$$g_{amp}(K_R \ or \ \psi_a) = 20 \log_{10}\left[abs\,(\overline{R}_{us} + i \,.\, I_{us}) \right]$$

$$- 20 \log_{10}\left[abs\,(\overline{R}_{di} + i \,.\, \overline{I}_{di}) \right] = 0 \qquad \text{(a-1)}$$

A decibel scale is used as is common in representing amplitude.

Matching the phase angle is equivalent to the following relation:

$$g_{phase}(K_R \ or \ \psi_a)\ ar\cos\left[\frac{\overline{R}_{us} \,.\, \overline{R}_{di} + \overline{I}_{us} \,.\, \overline{I}_{di}}{abs\,(\overline{R}_{us} + i \,.\, \overline{I}_{us}) \,.\, abs\,(\overline{R}_{di} + i \,.\, \overline{I}_{di})} \right] = 0 \qquad \text{(a-2)}$$

Each of the last two equations can be solved to obtain a value of K_R or ψ_a that satisfies this equation. In general it is not possible to satisfy both equations simultaneously by choosing a certain value of K_R or ψ_a. Thus one is faced with a typical least-squares problem where the number of equations exceeds the number of unknowns.

Moreover, at a certain frequency, (ω, the above two equations apply for each of the response variables. Therefore, at each frequency (a system of the following eight equations is obtained:

$$\left.\begin{array}{l} W^j_{amp} \,.\, g^j_{amp}(\omega, K_R \ or \ \psi_a) = 0 \\ W^j_{phase} \,.\, g^j_{pahse}(\omega, K_R \ or \ \psi_a) = 0 \end{array}\right\} j = 1 - 4 \qquad \text{(a-3)}$$

j indicates which one of the response variables is considered: q_f/lon, q_f/lat, p_f/lat or p_f/lon. W^j_{amp} and W^j_{phase} are weighting parameters that define the "relative importance of each of the equations".

Equation (a-3) indicates that at each frequency there are eight equations and only a single unknown, K_R or ψ_a. The situation is even more complicated if one would like to match the response along a certain range of perturbation frequencies. In order to do that it is necessary to define discrete frequencies that are distributed along the range of frequencies, and eight equations are defined at each one of these frequencies. Thus, if there are N_f such frequencies, one ends up with (8. N_f) equations, but still one unknown.

Many methods exist for solving least-squares problems, and there are many codes that are based on these methods. In the present analysis the subroutine BCLSF of the IMSL MATH library is used. This subroutine solves a nonlinear least squares problem, subject to bounds on the variables, using a modified Levenberg-Marquardt [70, 71] algorithm and a finite-difference Jacobian.

Table-1 : Aerodynamic phase lag vs. air speeds from various studies

	Hover	30 kts	40 kts	50 kts	60 kts	80 kts	100 kts
UH-60 (ε = 0.047)							
Takahashi (1995)	36						
Fletcher and Tischler (1997)	44.4						
Schulein (2001)	44	39	34	23		14	
AH-64 (ε = 0.038)							
Mansur and Tischler (1996)	36				19		
SBMR (ε = 0.09)							
Tischler (1999)			18.73				12.13
S-92 (ε = 0.047)							
Tischler et.al.(2001)	45						

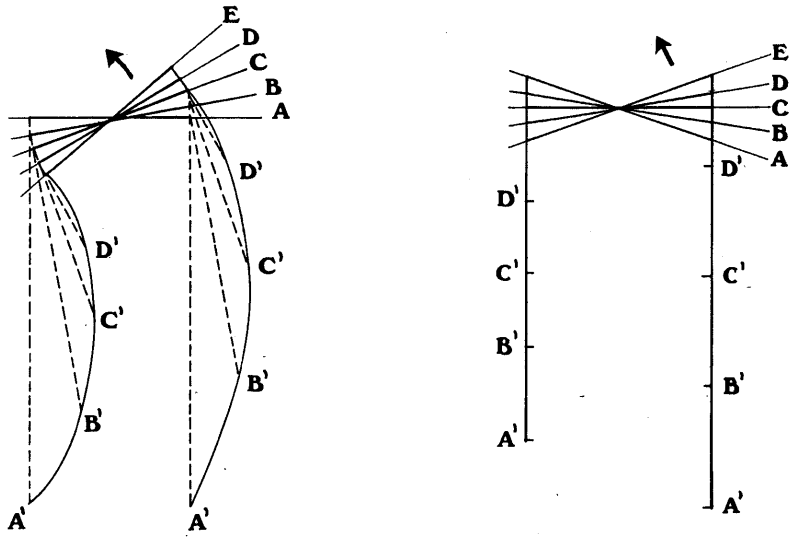

a) Each vortex element velocity is normal to the disk at the moment of departure

b) Each vortex element velocity is in the axial direction of the basic state.

Fig. 1 the wake distortion during a steady pitch in hover. For simplicity a constant induced velocity is assumed and contraction is neglected: the letters with an upper prime indicate a vortex element that departed from the disk at the orientation indicated by the same letter without a prime.

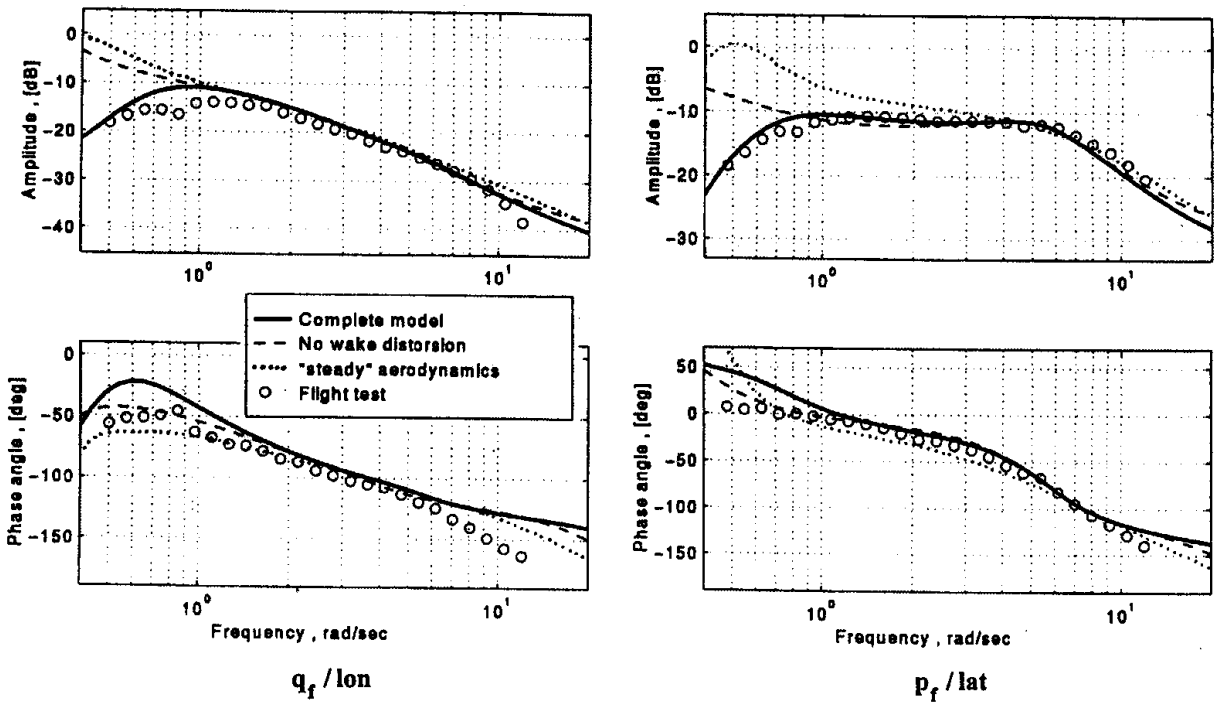

Fig. 2a. Frequency Response of an UH-60 in hover - Comparison between various results of TEMURA and flight-test results: On-axis response

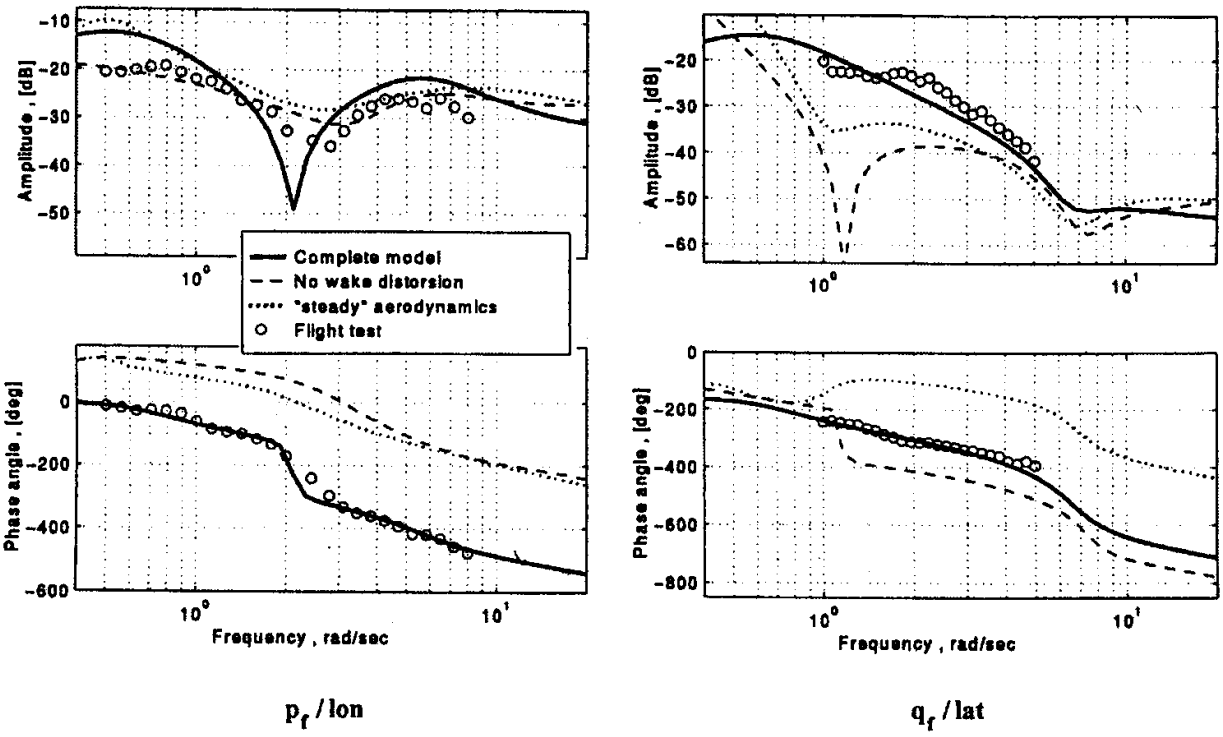

Fig. 2b. Frequency response of an UH-60 in hover - Comparison between various results of TEMURA and flight-test results: Off-axis response

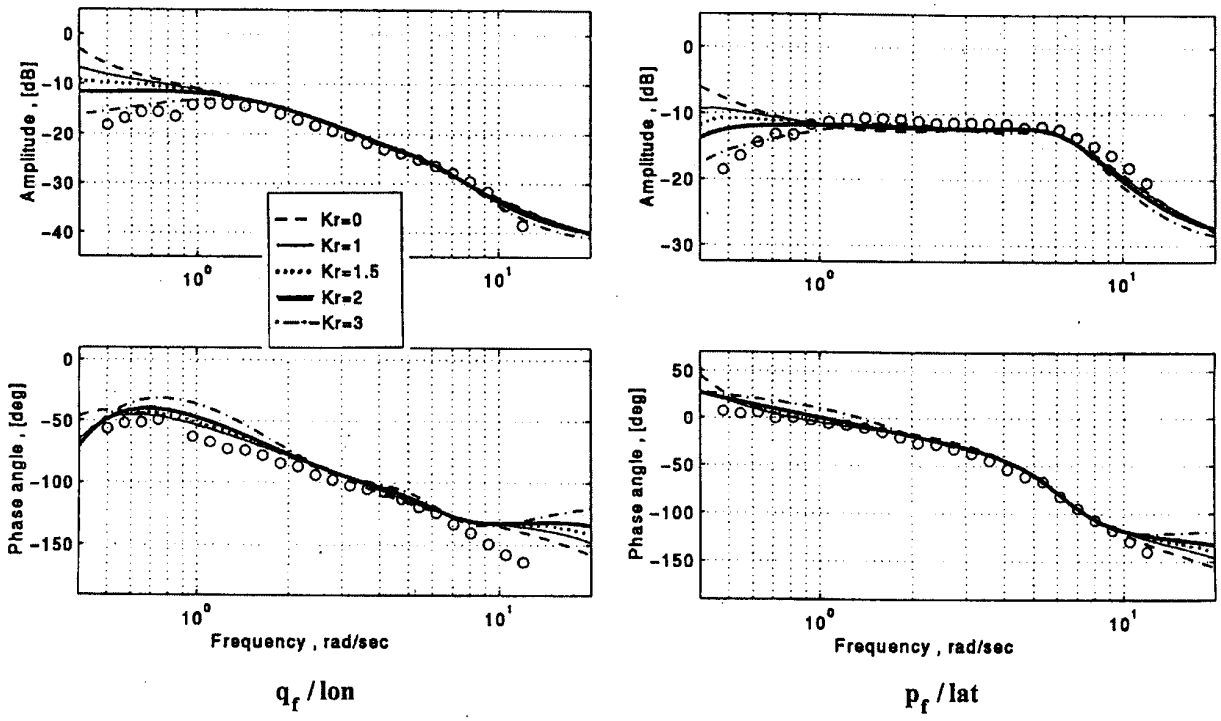

Fig. 3a. Frequency response of an UH-60 in hover - Results of a K_R correction: On-axis response

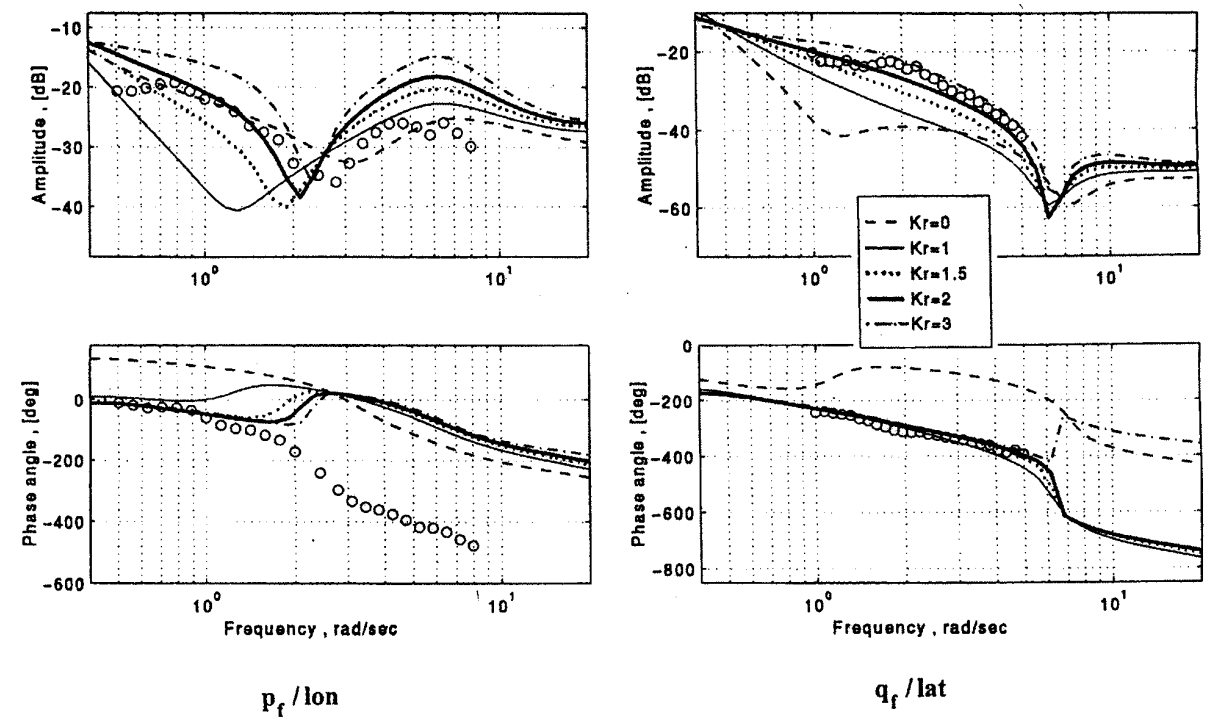

Fig. 3b. Frequency response of an UH-60 in hover - Results of a K_R correction: Off-axis response

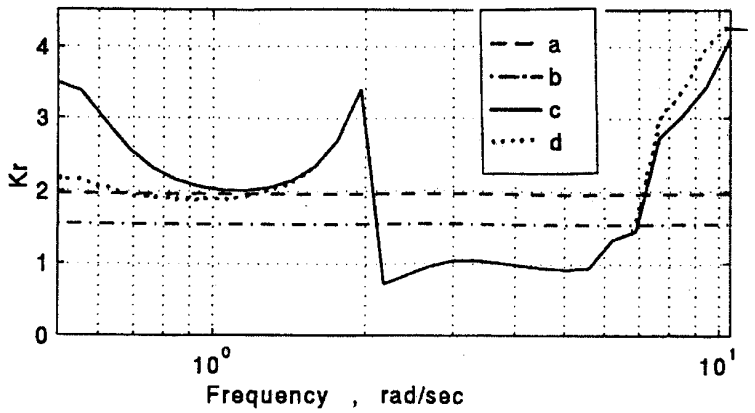

Fig. 4. Results of a least-squares procedure to find the optimal K_R value for an UH-60 in hover. a) Simultaneous matching of off-axis and on-axis responses in the entire range of frequencies. b) Simultaneous matching of off-axis responses only, in the entire range of frequencies. c) Matching the off-axis and on-axis response at each frequency. d) Matching the off-axis responses at each frequency

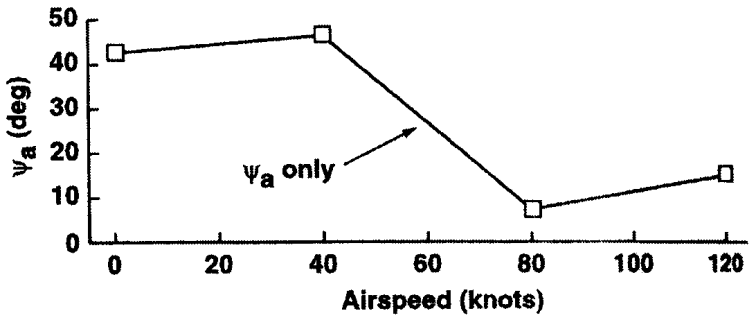

Fig. 5. The variation of the optimal as a function of the flight speed

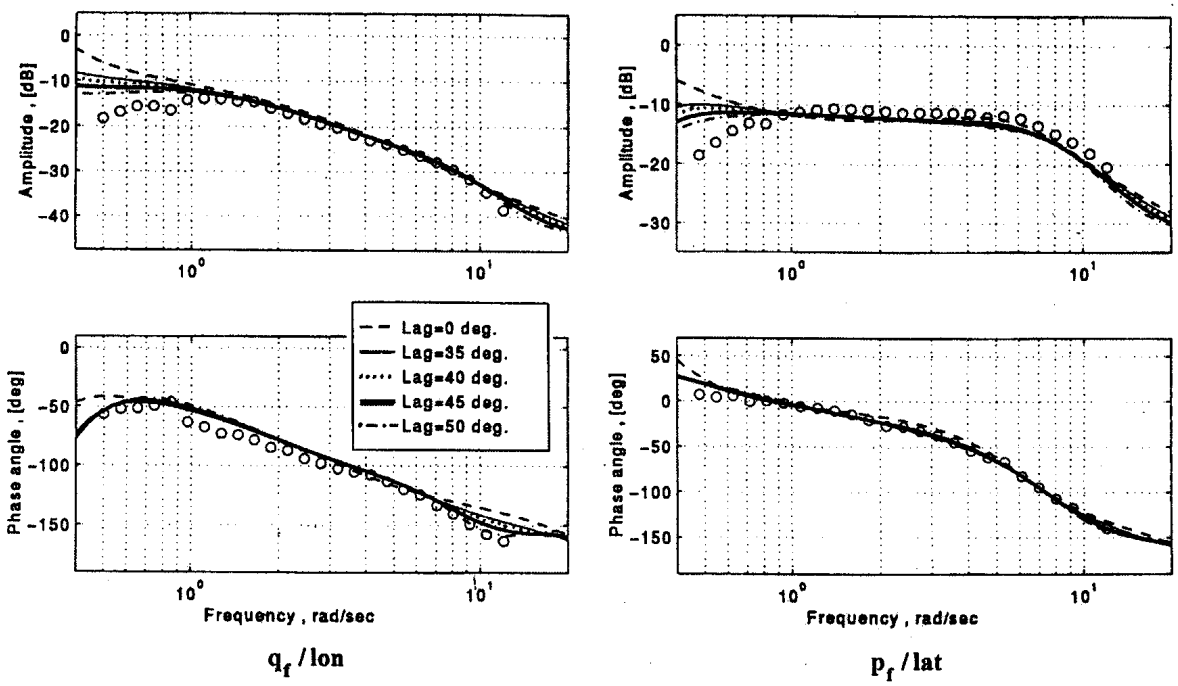

Fig. 6a. Frequency response of an UH-60 in hover - Results of a ψ_a correction: On-axis response

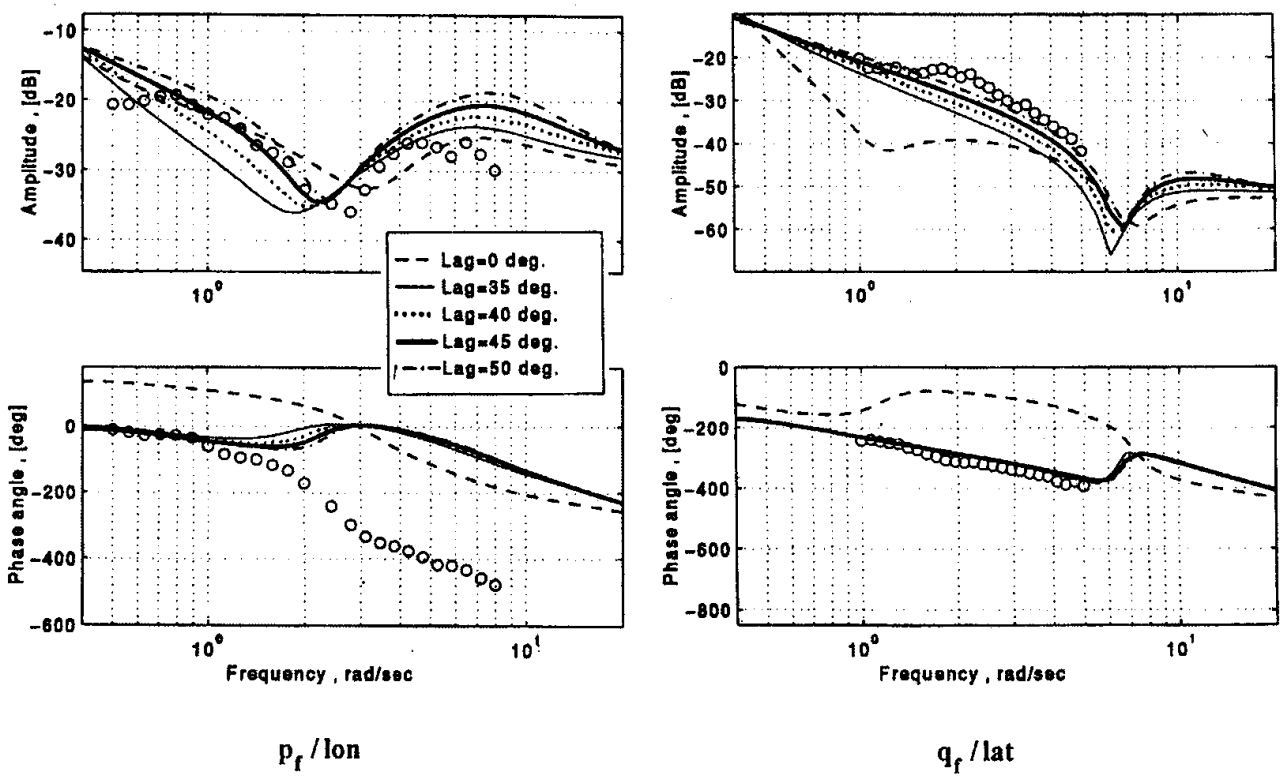

Fig. 6b. Frequency response of an UH-60 in hover - Results of a ψ_a correction: Off-axis response

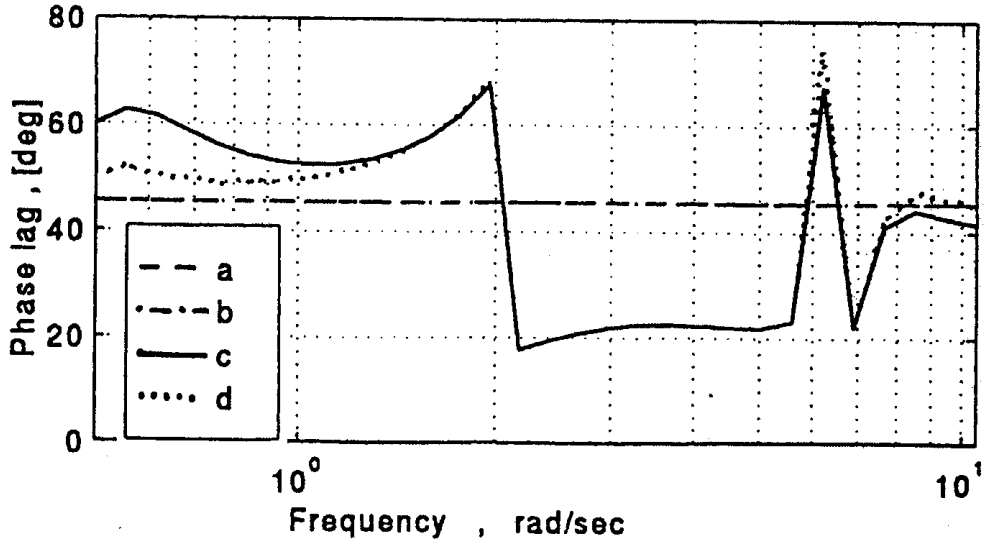

Fig. 7. Results of a least-square procedure to find the optimal value of an UH-60 in hover.
a) Simultaneous matching of off-axis and on-axis responses in the entire range of frequencies. b) Simultaneous matching of off-axis responses only, in the entire range of frequencies. c) Matching the off-axis and on-axis responses at each frequency. d) Matching the off-axis responses at each frequency

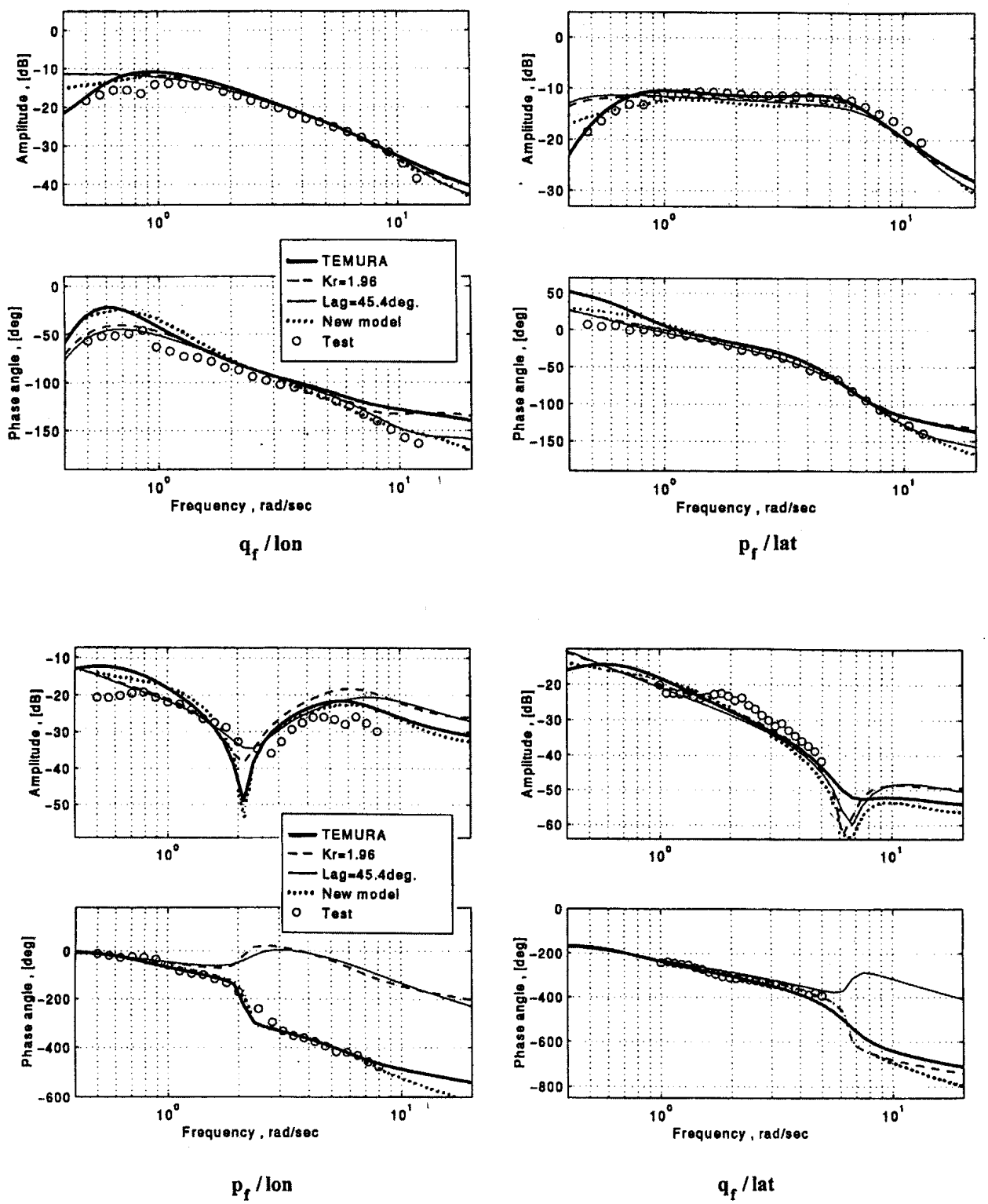

Fig. 8. Frequency response of an UH-60 in hover - Comparison between the results of TEMURA, the optimal K_R or ψ_a corrections, a new approximate actuator disk model and flight results

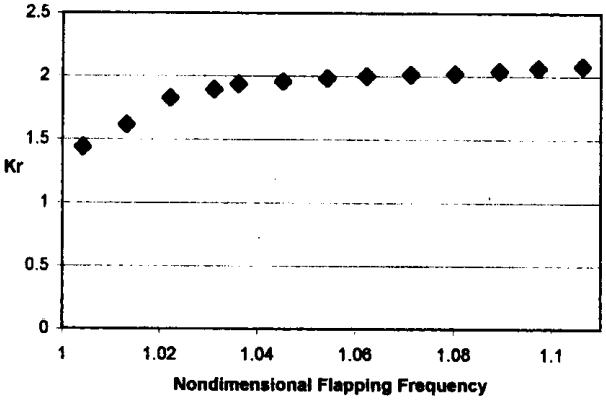

Fig. 9. The influence of the basic nondimensional flapping frequency on the optimal wake distortion coefficient, K_R, in hover

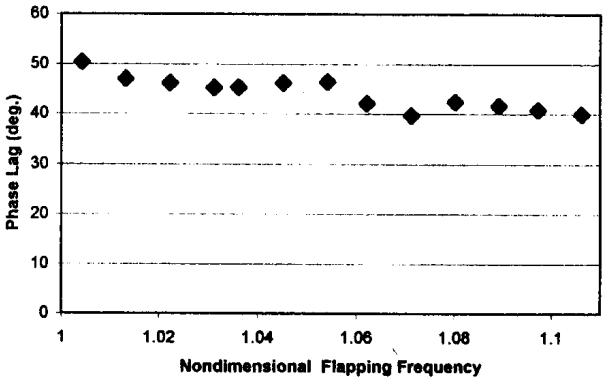

Fig. 10. The influence of the basic nondimensional flapping frequency on the optimal aerodynamic phase lag, ψ_a in hover

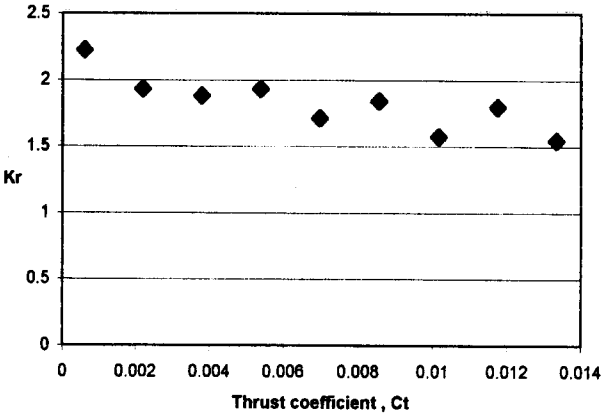

Fig. 11. The influence of thrust coefficient on the optimal wake distortion coefficient K_R, in hover

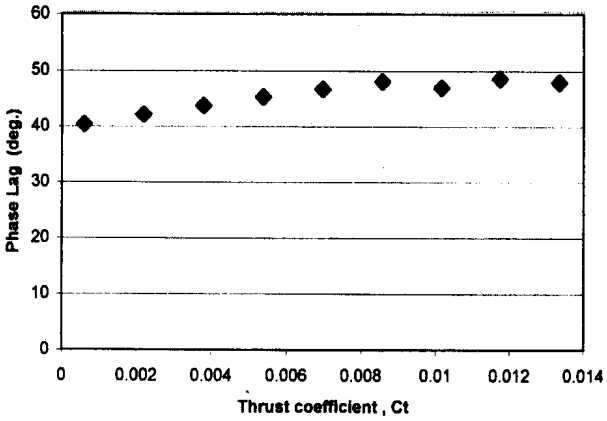

Fig. 12. The influence of thrust coefficient on the optimal aerodynamic phase lag, ψ_a in hover

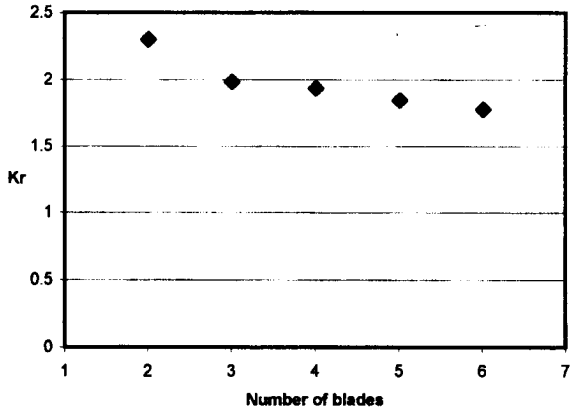

Fig. 13. The influence of the number of blades on the optimal wake distortion coefficient, K_R, in hover

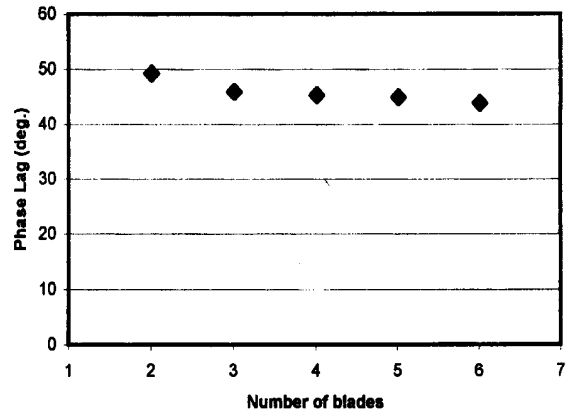

Fig. 14. The influence of the number of blades on the optimal aerodynamic phase lag, ψ_a , in hover